

1 **Source Apportionment of Fine Organic Carbon at an Urban Site of**
2 **Beijing using a Chemical Mass Balance Model**

3
4 **Jingsha Xu¹, Di Liu^{1,2}, Xuefang Wu^{1,3}, Tuan V. Vu^{1,4}, Yanli Zhang⁵, Pingqing Fu⁶, Yele Sun⁷, Weiqi**
5 **Xu⁷, Bo Zheng^{8,9}, Roy M. Harrison^{1,*}, Zongbo Shi^{1,*}**

6 1 School of Geography Earth and Environmental Science, University of Birmingham, Birmingham, B15 2TT, UK

7 2 Now at: Institute of Atmospheric Physics, Chinese Academy of Sciences, Beijing, 100029, China

8 3 School of Geology and Mineral Resources, China University of Geosciences Xueyuan Road 29, Beijing, 100083, China

9 4 Now at: Faculty of Life Sciences & Medicine, King's College London, London, WC2R 2LS, UK

10 5 Guangzhou Institute of Geochemistry, Chinese Academy of Sciences, Guangzhou, 510640, China

11 6 Institute of Surface-Earth System Science, Tianjin University, Tianjin, 300072, China

12 7 State Key Laboratory of Atmospheric Boundary Layer Physics and Atmospheric Chemistry, Institute of Atmospheric Physics,
13 Chinese Academy of Sciences, Beijing, 100029, China

14 8 State Key Joint Laboratory of Environment Simulation and Pollution Control, School of Environment, Tsinghua University,
15 Beijing, 100084, China

16 9 Now at: Laboratoire des Sciences du Climat et de l'Environnement, CEA-CNRS-UVSQ, UMR8212, Gif-sur-Yvette, France

18 ***Correspondence:** Zongbo Shi (Z.Shi@bham.ac.uk) and Roy Harrison (r.m.harrison@bham.ac.uk)

19 **Abstract**

20 Fine particles were sampled from 9th November to 11th December 2016 and 22nd May
21 to 24th June 2017 as part of the Atmospheric Pollution and Human Health in a Chinese
22 megacity (APHH-China) field campaigns in urban Beijing, China. Inorganic ions, trace
23 elements, OC, EC, and organic compounds including biomarkers, hopanes, PAHs, n-
24 alkanes and fatty acids, were determined for source apportionment in this study.
25 Carbonaceous components contributed on average 47.2% and 35.2% of total
26 reconstructed PM_{2.5} during the winter and summer campaigns, respectively. Secondary
27 inorganic ions (sulfate, nitrate, ammonium- SNA) accounted for 35.0% and 45.2% of
28 total PM_{2.5} in winter and summer. Other components including inorganic ions (K⁺, Na⁺,
29 Cl⁻), geological minerals, and trace metals only contributed 13.2% and 12.4% of PM_{2.5}
30 during the winter and summer campaigns. Fine OC was explained by seven primary
31 sources (industrial/residential coal burning, biomass burning, gasoline/diesel vehicles,
32 cooking and vegetative detritus) based on a chemical mass balance (CMB) receptor
33 model. It explained an average of 75.7% and 56.1% of fine OC in winter and summer,
34 respectively. Other (unexplained) OC was compared with the secondary OC (SOC)
35 estimated by the EC-tracer method, with correlation coefficients (R²) of 0.58 and 0.73,
36 and slopes of 1.16 and 0.80 in winter and summer, respectively. This suggests that the
37 unexplained OC by CMB was mostly associated with SOC. PM_{2.5} apportioned by CMB
38 showed that the SNA and secondary organic matter were the highest two contributors
39 to PM_{2.5}. After these, coal combustion and biomass burning were also significant
40 sources of PM_{2.5} in winter. The CMB results were also compared with results from
41 Positive Matrix Factorization (PMF) analysis of co-located Aerosol Mass Spectrometer
42 (AMS) data. The CMB was found to resolve more primary OA sources than AMS-PMF
43 but the latter could apportion secondary OA sources. The AMS-PMF results for major
44 components, such as coal combustion OC and oxidized OC correlated well with the
45 results from CMB. However, discrepancies and poor agreements were found for other
46 OC sources, such as biomass burning and cooking, some of which were not identified
47 in AMS-PMF factors.

51

52 **Keywords:** PM_{2.5}, Beijing, mass closure, CMB, AMS-PMF, source apportionment

53 **1 Introduction**

54 Beijing is the capital of China and a hotspot of particulate matter pollution. It has been
55 experiencing severe PM_{2.5} (particulate matter with an aerodynamic diameter of
56 $\leq 2.5 \mu\text{m}$) pollution in recent decades, as a result of rapid urbanization and
57 industrialization, and increasing energy consumption (Wang et al., 2009). High PM_{2.5}
58 pollution from Beijing could have significant impact on human health (Song et al.,
59 2006a; Li et al., 2013). A case study in Beijing revealed that a 10 $\mu\text{g m}^{-3}$ increase of
60 ambient PM_{2.5} concentration will correspondingly increase 0.78%, 0.85% and 0.75%
61 of the daily mortality of the circulatory diseases, cardiovascular diseases and
62 cerebrovascular diseases, respectively (Dong et al., 2013). Furthermore, PM_{2.5} causes
63 visibility deterioration in Beijing. A better understanding of PM_{2.5} sources in Beijing is
64 essential, as it can provide important scientific evidence to develop measures to control
65 PM_{2.5} pollution.

66 Many studies have identified the possible sources of fine particulate matter in Beijing
67 using various methods (Zheng et al., 2005; Song et al., 2006a; Song et al., 2006b; Li et
68 al., 2015; Zhang et al., 2013; Yu and Wang, 2013). Song et al. (2006a) applied
69 two eigenvector models, principal component analysis/absolute principal component
70 scores (PCA/APCS) and UNMIX to study the sources of PM_{2.5} in Beijing. Some studies
71 used elemental tracers to do source apportionment of PM_{2.5} by applying positive matrix
72 factorization (PMF) (Song et al., 2006b; Li et al., 2015; Zhang et al., 2013; Yu and
73 Wang, 2013). This approach has some underlying challenges. For example, PMF
74 requires a relatively large sample size and a “best” solution of achieved factors requires
75 critical assessment of its mathematical parameters and evaluation of the physical
76 reasonability of the factor profiles (de Miranda et al., 2018; Ikemori et al., 2021; Oduber
77 et al., 2021); secondly, many important PM_{2.5} emission sources do not have a unique
78 elemental composition. Hence, an elemental tracer-based method cannot distinguish
79 sources such as cooking or vehicle exhaust, as they emit mainly carbonaceous
80 compounds (Wang et al., 2009). Generally, organic matter (OM) is composed of
81 primary organic matter (POM) and secondary organic matter (SOM). POM is directly
82 emitted and SOM is formed through chemical oxidation of volatile organic compounds
83 (VOCs) (Yang et al., 2016). OM was the largest contributor to PM_{2.5} mass, which was
84 reported to account for 30%-50% of PM_{2.5} in some Chinese cities such as Beijing,
85 Guangzhou, Xi'an and Shanghai (Song et al., 2007; He et al., 2001; Huang et al., 2014),
86 and can contribute up to 90% of submicron PM mass in Beijing (Zhou et al., 2018).
87 Furthermore, many organic tracers are more specific to particular sources, making them
88 more suitable to identify and quantify different source contributions to carbonaceous
89 aerosols and PM_{2.5}.

90 Chemical Mass balance (CMB) model has been used for source apportionment of
91 PM worldwide, including in the US (Antony Chen et al., 2010), UK (Yin et al., 2015),
92 and China (Chen et al., 2015b). The CMB model assumes that source profiles remain
93 unchanged between the emitter and receptor (Sarnat et al., 2008; Viana et al., 2008). Xu
94 et al. (2021) compared the source apportionment results of fine particles by multiple
95 receptor modelling approaches, and found that CMB can provide the most complete
96 and representative source apportionment of Beijing aerosols. A few studies have applied
97 a CMB model for source apportionment of PM in Beijing (Zheng et al., 2005; Liu et al.,
98 2016; Guo et al., 2013; Wang et al., 2009). For example, Zheng et al. (2005) investigated

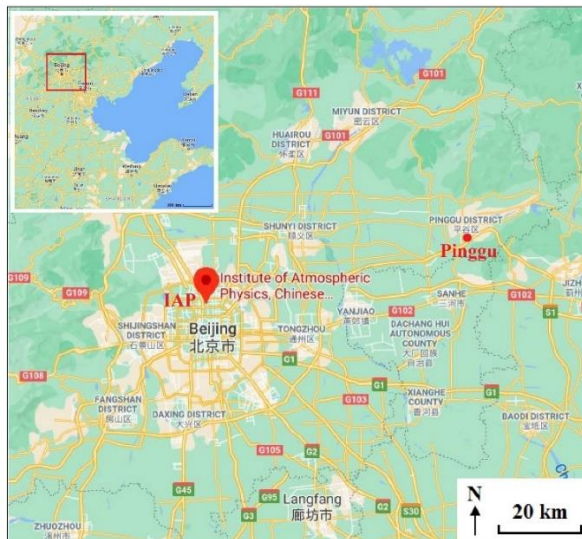
99 sources of $\text{PM}_{2.5}$ in Beijing, but the source profiles they used were mainly derived in
100 the United States, which were less representative of the local sources. Liu et al. (2016)
101 and Guo et al. (2013) apportioned the sources of $\text{PM}_{2.5}$ in a typical haze episode in
102 winter 2013 in Beijing during the Olympic Games period in summer 2008, respectively.
103 Wang et al. (2009) apportioned the sources of $\text{PM}_{2.5}$ in both winter and summer. A major
104 challenge of the CMB model is that it cannot quantify the contributions of secondary
105 organic aerosol and unknown sources, which are often lumped as “unexplained OC”.

106 In this study, $\text{PM}_{2.5}$ samples were collected at an urban site of Beijing in winter 2016
107 and summer 2017. OC, EC, PAHs, alkanes, hopanes, fatty acids and monosaccharide
108 anhydrides in the $\text{PM}_{2.5}$ samples were determined, and applied in the CMB model for
109 apportioning the organic carbon sources. To ensure that the source profiles used in the
110 CMB model are representative, we mainly selected data which had been determined in
111 China. The objectives of this study are: 1) to quantify the contributions of pollution
112 sources to OC by applying a CMB model and compare them with those at a rural site
113 of Beijing; 2) to compare the source apportionment results by CMB with those from
114 Aerosol Mass Spectrometer-PMF analysis (AMS-PMF), to improve our understanding
115 of different sources of OC.

116 2 Methodology

117 2.1 Aerosol sampling

118 $\text{PM}_{2.5}$ was collected at an urban sampling site (116.39E, 39.98N) - the Institute of
119 Atmospheric Physics (IAP) of the Chinese Academy of Sciences in Beijing, China from
120 9th November to 11th December 2016 and 22nd May to 24th June 2017, as part of the
121 Atmospheric Pollution and Human Health in a Chinese megacity (APHH-China) field
122 campaigns (Shi et al., 2019). The sampling site (Fig. 1) is located in the middle between
123 the North 3rd Ring Road and North 4th Ring Road and approximately 200 m from a
124 major highway. Hence, it is subject to many local sources, such as traffic, cooking, etc.
125 The location of a rural site in Beijing - Pinggu during the APHH-China campaigns is
126 also shown in Fig. 1. The rural site in Xibaidian village in Pinggu is about 60 km away
127 from IAP and 4 km north-west of the Pinggu town centre. It is surrounded by trees and
128 farmland with several similar small villages nearby. A provincial highway is
129 approximately 500 m away on its eastside running north-south. This site is far from
130 industrial sources and located in a residential area. Other information regarding the
131 sampling site is described elsewhere (Shi et al., 2019).



132

133 **Figure 1.** Locations of the sampling sites in Beijing (IAP - urban site: Institute of Atmospheric Physics
 134 of the Chinese Academy of Sciences; Pinggu - rural site) (source: © Google Maps).

135 PM_{2.5} samples were collected on pre-baked (450°C for 6h) large quartz filters
 136 (Pallflex, 8×10 inch) by Hi-Vol air sampler (Tisch, USA) at a flow rate of 1.1 m³ min⁻¹. A Medium-Vol air sampler (Thermo Scientific Partisol 2025i) was also deployed at
 137 the same location to collect PM_{2.5} samples simultaneously on 47 mm PTFE filters at a
 138 flow rate of 15.0 L min⁻¹. Field blanks were also collected with the pump turned off
 139 during the sampling campaign. Before and after sampling, all filters were put in a
 140 balance room and equilibrated at a constant temperature and relative humidity (RH) for
 141 24h prior to any gravimetric measurements, which were 22°C and 30% RH for summer
 142 samples, 21°C and 33% RH for winter samples. PM_{2.5} mass was determined through
 143 the weighing of PTFE filters using a microbalance (Sartorius model MC5, precision: 1
 144 µg). After that, filters were wrapped separately with aluminum foil and stored at under
 145 -20°C in darkness until analysis. The large quartz filters were analyzed for OC, EC,
 146 organic compounds and ion species, while small PTFE filters were used for the
 147 determination of PM_{2.5} mass and metals. Online PM_{2.5} were determined by the TEOM
 148 FDMS 1405-DF instrument at IAP with filter equilibrating and weighing conditions
 149 comparable with the United States Federal Reference Method (RH: 30-40%;
 150 temperature; 20-23°C) (Le et al., 2020; U.S.EPA, 2016).
 151

152 **2.2 Chemical Analysis**

153 **2.2.1 OC and EC**

154 A 1.5 cm² punch from each large quartz filter sample was taken for organic carbon (OC)
 155 and elemental carbon (EC) measurements by a thermal/optical carbon analyzer (model
 156 RT-4, Sunset Laboratory Inc., USA) based on the EUSAAR2 (European Supersites for
 157 Atmospheric Aerosol Research) transmittance protocol (Cavalli et al., 2010; Chen et al.,
 158 2015a). Replicate analyses of OC and EC were conducted once every ten samples. The
 159 uncertainties from duplicate analyses of filters were <10%. All sample results were
 160 corrected by the values obtained from field blanks, which were 0.40 and 0.01 µg m⁻³
 161 for OC and EC, respectively. Details of the OC/EC measurement method can be found
 162 elsewhere (Paraskevopoulou et al., 2014). The instrumental limits of detection of OC

163 and EC in this study were estimated to be 0.03 and 0.05 $\mu\text{g m}^{-3}$, respectively.

164

165 2.2.2 Organic compounds

166 Organic tracers, including 11 n-alkanes (C₂₄-C₃₄), 2 hopanes (17a (H) -22, 29, 30-
167 Trisnorhopane, 17b (H), 21a (H) -Norhopane), 17 PAHs (retene, phenanthrene,
168 anthracene, fluoranthene, pyrene, benz(a)anthracene, chrysene, benzo(b)fluoranthene,
169 benzo(k)fluoranthene, benzo(e)pyrene, benzo(a)pyrene, perylene, Indeno(1,2,3-
170 cd)pyrene, dibenz(a,h)anthracene, benzo(ghi)perylene, coronene, picene), 3
171 anhydrosugars (levoglucosan, mannosan, galactosan), 2 fatty acids (palmitic acid,
172 stearic acid) and cholesterol in the PM_{2.5} samples were determined in this study. 9 cm^2
173 of the large quartz filters were extracted 3 times with dichloromethane/methanol (HPLC
174 grade, v/v: 2:1) under ultrasonication for 10 minutes. The extracts were then filtered
175 and concentrated using a rotary evaporator under vacuum, and blown down to dryness
176 with pure nitrogen gas. 50 μL of N,O-bis-(trimethylsilyl)trifluoroacetamide (BSTFA)
177 with 1% trimethylsilyl chloride and 10 μL of pyridine were then added to the extracts,
178 which were left reacting at 70 °C for 3 h to derivatize -COOH to TMS esters and -OH
179 to TMS ethers. After cooling to room temperature, the derivatives were diluted with
180 140 μL of internal standards (C13 n-alkane, 1.43 ng μL^{-1}) in n-hexane prior to GC-MS
181 analysis. The final solutions were analyzed by a gas chromatography mass spectrometry
182 system (GC/MS, Agilent 7890A GC plus 5975C mass-selective detector) fitted with a
183 DB-5MS column (30 m × 0.25 mm × 0.25 μm). The GC temperature program and MS
184 detection details were reported in Li et al. (2018). Individual compounds were identified
185 through the comparison of mass spectra with those of authentic standards or literature
186 data (Fu et al., 2016). Recoveries for these compounds were in a range of 70-100%,
187 which were obtained by spiking standards to pre-baked blank quartz filters followed by
188 the same extraction and derivatization procedures. Field blank filters were analyzed the
189 same way as samples for quality assurance, but no target compounds were detected.

190 2.2.3 Inorganic components

191 Half of the PTFE filter was extracted with 10 mL ultrapure water for the analysis of
192 inorganic ions. Major inorganic ions including Na⁺, K⁺, NH₄⁺, Cl⁻, NO₃⁻ and SO₄²⁻ were
193 determined by using an ion chromatograph (IC, Dionex, Sunnyvale, CA, USA), the
194 detection limits (DLs) of them were 0.032, 0.010, 0.011, 0.076, 0.138, 0.240 and 0.142
195 $\mu\text{g m}^{-3}$ respectively. The analytical uncertainty was less than 5% for all inorganic ions.
196 An intercomparison study showed that our IC analysis of the above-mentioned ions
197 agreed well with those of the other laboratories (Xu et al., 2020). Trace metal including
198 Al (DLs in $\mu\text{g m}^{-3}$, 0.221), Si (0.040), Ca (0.034), Ti (0.003) and Fe (0.044) were
199 determined by X-ray fluorescence spectrometer (XRF). Other elements including V, Cr,
200 Co, Mn, Ni, Cu, Zn, As, Sr, Cd, Sb, Ba and Pb were analyzed by Inductively-coupled
201 plasma-mass spectrometer (ICP-MS) after extraction of 1/2 PTFE filter by diluted acid
202 mixture (HNO₃/HCl), and the detection limits of them were 1.32, 0.25, 0.04, 0.06, 2.05,
203 1.25, 1.22, 1.74, 0.02, 0.03, 0.11, 0.06 and 0.04 ng m^{-3} , respectively. Mass
204 concentrations of all inorganic ions and elements in this study were corrected for the
205 field blank values, and the methods were quality assured with standard reference
206 materials.

207

208 **2.3 Chemical Mass Closure (CMC) Method**

209 A Chemical Mass Closure analysis was carried out, which includes secondary inorganic
210 ions (sulfate, nitrate, ammonium; SNA), sodium, potassium and chloride salts,
211 geological minerals, trace elements, organic matter (OM), EC and bound water in
212 reconstructed PM_{2.5}. Geological minerals were calculated applying the equation (Eq. 1)
213 (Chow et al., 2015):

214 Geological minerals = 2.2Al + 2.49Si + 1.63Ca + 1.94Ti + 2.42Fe (1)

215 Trace elements were the sum of all analysed elements excluding Al, Si, Ca, Ti and
216 Fe. The average OM/OC ratios of organic aerosols (OA) from AMS elemental analysis
217 were applied to calculate OM, which were 1.75±0.16 and 2.00±0.19 in winter and
218 summer, respectively. Based on the concentrations of inorganic ions and gas-phase NH₃,
219 particle bound water was calculated by ISORROPIA II model (available
220 at <http://isorropia.eas.gatech.edu>) in forward mode and thermodynamically metastable
221 phase state (Fountoukis and Nenes, 2007). Two sets of calculations were done for online
222 and offline data, differing at the temperature and relative humidity as specified above.

223 **2.4 Chemical Mass Balance (CMB) model**

224 The chemical mass balance model (US EPA CMB8.2) was applied in this study to
225 apportion the sources of OC by utilizing a linear least squares solution. Both
226 uncertainties in source profiles and ambient measurements were taken into
227 consideration in this model. The source profiles applied here were from local studies in
228 China to better represent the source characteristics, including straw burning (wheat,
229 corn, rice straw burning) (Zhang et al., 2007b), wood burning (Wang et al., 2009),
230 gasoline and diesel vehicles (including motorcycles, light- and heavy-duty gasoline and
231 diesel vehicles) (Cai et al., 2017), industrial and residential coal combustion (including
232 anthracite, sub-bituminite, bituminite, and brown coal) (Zhang et al., 2008), and
233 cooking (Zhao et al., 2015), except vegetative detritus (Rogge et al., 1993; Wang et al.,
234 2009). The source profiles with EC and organic tracers used in the CMB model were
235 provided in Table S1 of Wu et al. (2020). The selected fitting species were EC,
236 levoglucosan, palmitic acid, stearic acid, fluoranthene, phenanthrene, retene,
237 benz(a)anthracene, chrysene, benzo(b)fluoranthene, benzo(k)fluoranthene,
238 benzo[ghi]perylene, picene, 17a (H) -22, 29, 30-trisnorhopane, 17b (H), 21a (H) -
239 norhopane and n-alkanes (C24-C33), the concentrations of which are provided in Table
240 1. The essential criteria in this model were met to ensure reliable fitting results. For
241 instance, in all samples, R² were >0.80 (mostly >0.9), Chi² were <2, T_{stat} values were
242 mostly greater than 2 except the source of vegetative detritus, and C/M ratios (ratio of
243 calculated to measured concentration) for all fitting species were in range of 0.8-1.2 in
244 this study.

245

246 **2.5 Positive Matrix Factorization analysis of data obtained from Aerosol Mass
247 Spectrometer (AMS-PMF)**

248 An Aerodyne AMS with a PM₁ aerodynamic lens was deployed on the roof of the
249 neighboring building- the Tower branch of IAP for real-time measurements of non-

250 refractory (NR) chemical species from 16th November to 11th December 2016 and 22nd
251 May to 24th June 2017. The detailed information of the sampling sites is given
252 elsewhere (Xu et al., 2019b). The submicron particles were dried and sampled into the
253 AMS at a flow of ~0.1 L min⁻¹. NR-PM₁ can be quickly vaporized by the 600 °C
254 tungsten vaporizer and then the NR-PM₁ species including organics, Cl⁻, NO₃⁻, SO₄²⁻
255 and NH₄⁺ were measured by AMS in mass sensitive V mode (Sun et al., 2020). Details
256 of AMS data analysis, including the analysis of organic aerosol (OA) mass spectra can
257 be found elsewhere (Xu et al., 2019b). The source apportionment of organics in NR-
258 PM₁ was carried out by applying PMF to the high-resolution mass spectra of OA, while
259 that of fine OC in this study was conducted by applying source profiles along with an
260 offline chemical speciation dataset. The procedures of the pretreatment of spectral data
261 and error matrices can be found elsewhere (Ulbrich et al., 2009). It is noted that the data
262 were missing during the period 09th - 15th November 2016 due to the malfunction of the
263 AMS.

264

265 3 Results and discussion

266 3.1 Characteristics of PM_{2.5} and Carbonaceous Compounds

267 Mean concentrations of PM_{2.5}, OC, EC and organic tracers during wintertime (9th
268 November to 11th December 2016) and summertime (22nd May to 24th June 2017) at the
269 IAP site are summarized in Table 1 and Fig. S1. The average PM_{2.5} concentration was
270 94.8±64.4 $\mu\text{g m}^{-3}$ during the whole winter sampling campaign. The winter sampling
271 period was divided into haze (daily PM_{2.5} > 75 $\mu\text{g m}^{-3}$) and non-haze days (<75 $\mu\text{g m}^{-3}$),
272 based on the National Ambient Air Quality Standard Grade II of the limit for 24-
273 hour average PM_{2.5} concentration. The differentiation between haze and non-haze days
274 enabled us to study the major sources contributing to the haze formation. The average
275 daily PM_{2.5} was 136.7±49.8 and 36.7±23.5 $\mu\text{g m}^{-3}$ on haze and non-haze days,
276 respectively. Daily PM_{2.5} in the summer sampling period was 30.2±14.8 $\mu\text{g m}^{-3}$,
277 comparable with that on winter non-haze days.

278 OC concentrations ranged between 3.9-48.8 $\mu\text{g m}^{-3}$ (mean: 21.5 $\mu\text{g m}^{-3}$) and 1.8-12.7
279 $\mu\text{g m}^{-3}$ (mean: 6.4 $\mu\text{g m}^{-3}$) during winter and summer, respectively. They are
280 comparable with the OC concentrations in winter (23.7 $\mu\text{g m}^{-3}$) and summer (3.78 $\mu\text{g m}^{-3}$)
281 in Tianjin, China during an almost simultaneous sampling period (Fan et al., 2020),
282 but much lower than the OC concentration (17.1 $\mu\text{g m}^{-3}$) in summer 2007 in Beijing
283 (Yang et al., 2016). The average OC concentration during haze days (29.4±9.2 $\mu\text{g m}^{-3}$)
284 was approximately three times that of non-haze days (10.7±6.2 $\mu\text{g m}^{-3}$) during winter.
285 The average EC concentration during winter was 3.5±2.0 $\mu\text{g m}^{-3}$; its concentration was
286 4.6±1.3 $\mu\text{g m}^{-3}$ on haze days, approximately 2.4 times that on winter non-haze days
287 (1.9±1.6 $\mu\text{g m}^{-3}$) and 5 times that (0.9±0.4 $\mu\text{g m}^{-3}$) during the summer sampling period.
288 The OC and EC concentrations in this study were comparable with the OC (27.9 ± 23.4
289 $\mu\text{g m}^{-3}$) and EC (6.6 ± 5.1 $\mu\text{g m}^{-3}$) concentrations in winter Beijing in 2016 (Qi et al.,
290 2018), but much lower than those in an urban area of Beijing during winter (OC and
291 EC: 36.7±19.4 and 15.2±11.1 $\mu\text{g m}^{-3}$) and summer (10.7±3.6 and 5.7±2.9 $\mu\text{g m}^{-3}$) in
292 2002 (Dan et al., 2004).

293 On average, OC and EC concentrations in winter were 3.3 and 3.9 times those in
 294 summer. Additionally, OC and EC were well-correlated in this study, with R^2 values of
 295 0.85 and 0.63 during winter and summer, respectively, suggesting similar paths of OC
 296 and EC dispersion and dilution, and/or similar sources of carbonaceous aerosols, especially
 297 in winter. Less correlated OC and EC in summer could be a result of SOC formation.
 298 SOC in this study was estimated and is discussed in section 3.3.7.

299 **Table 1.** Summary of measured concentrations at IAP site in winter and summer.

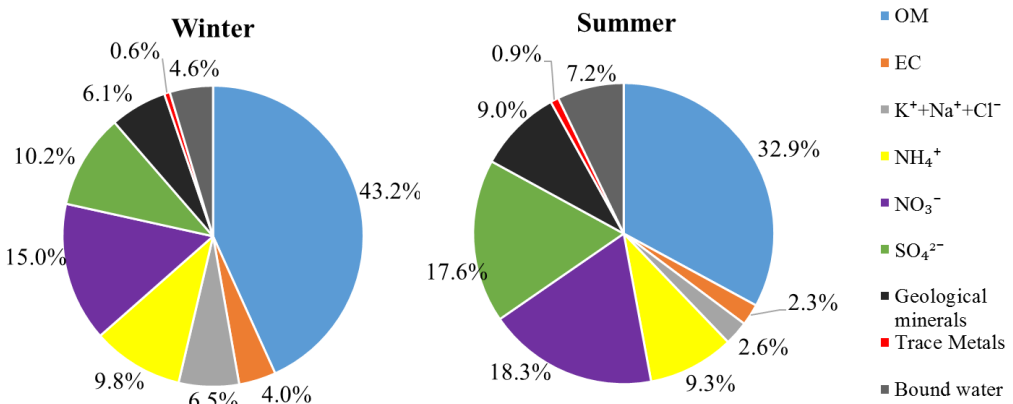
Compounds ^a / ng m ⁻³	Winter		Winter (n=31)	Summer (n=34)
	Haze ^d (n=18)	Non-haze ^e (n=13)		
PM _{2.5} (μg m ⁻³)	136.7±49.8 (80.5-239.9) ^b	36.7±23.5 (10.3-72)	94.8±64.4 (10.3-239.9)	30.2±14.8 (12.2-78.8)
OC (μg m ⁻³)	29.4±9.2 (13.7-48.8)	10.7±6.2 (3.9-21.5)	21.5±12.3 (3.9-48.8)	6.4±2.3 (1.8-12.7)
EC (μg m ⁻³)	4.6±1.3 (1.6-6.6)	1.9±1.6 (0.3-5.2)	3.5±2.0 (0.3-6.6)	0.9±0.4 (0.2-1.7)
SOC ^c (μg m ⁻³)	10.3±5.7 (2.9-24.6)	2.9±1.4 (0.0-5.5)	7.2±5.7 (0.0-24.6)	2.3±1.4 (0.0-6.0)
Levoglucosan	348.2±148.0 (83.1-512.5)	195.0±163.7 (19.1-539.5)	278.5±171.4 (19.1-539.5)	26.1±28.3 (2.9-172.2)
Palmitic acid	376.2±234.9 (44.5-1089.6)	278±280.6 (33.8-1137.2)	335±255.3 (33.8-1137.2)	25.2±11.9 (9.4-68)
Stearic acid	207.1±181.4 (23-846.7)	163.6±228.1 (17.3-903.2)	188.8±199.8 (17.3-903.2)	16.0±7.2 (5.6-36.4)
Phenanthrene	8.6±6.1 (1.8-19)	5.6±6.1 (1-24.8)	7.3±6.2 (1-24.8)	0.7±0.7 (0-3.8)
Fluoranthene	25.1±19.6 (4.2-76.2)	16.1±21.3 (4.2-84.3)	21.3±20.5 (4.2-84.3)	0.4±0.2 (0-0.9)
Retene	16±14.9 (2-52.2)	11.1±12.1 (0.5-45.5)	13.9±13.8 (0.5-52.2)	0±0 (0-0.1)
Benz(a)anthracene	21.5±16.5 (0.3-62.7)	10.8±9.3 (1.4-30.5)	17±14.8 (0.3-62.7)	0.2±0.1 (0-0.5)
Chrysene	22.6±14.1 (3.7-47.3)	13.6±15.6 (0.1-59.5)	18.8±15.2 (0.1-59.5)	0.2±0.1 (0-0.3)
Benzo(b)fluoranthene	52.6±29 (10.7-98)	28.1±31 (2.4-113.6)	42.3±31.8 (2.4-113.6)	0.7±0.5 (0-2)
Benzo(k)fluoranthene	12.2±8 (0-25.3)	6.7±6.8 (0-23.7)	9.9±7.9 (0-25.3)	0.2±0.1 (0-0.4)
Picene	0.8±0.8 (0-2.6)	0.3±0.5 (0-1.3)	0.6±0.7 (0-2.6)	0±0 (0-0)
Benzo(ghi)perylene	7.0±4.7 (0-13.6)	4.0±4.1 (0-14.0)	5.6±4.6 (0-14.0)	0±0.1 (0-0.3)
17a (H) -22, 29, 30- Trisnorhopane	2.7±1.6 (0.6-6.7)	1.6±1.5 (0.3-6)	2.2±1.6 (0.3-6.7)	0±0.1 (0-0.4)
17b (H), 21a (H) - Norhopane	3.1±1.6 (0.9-6.6)	1.8±1.8 (0.3-7.3)	2.6±1.8 (0.3-7.3)	0±0 (0-0.2)
C24	26.3±15.3 (7.8-55.5)	18±19.2 (2.1-71.2)	22.5±17.4 (2.1-71.2)	1.4±0.6 (0.5-3.3)
C25	28.2±15.6 (8.5-59)	19.5±20.5 (2.3-76.2)	24.2±18.3 (2.3-76.2)	2.9±1.5 (0.5-6.5)
C26	18.9±10.2 (5.8-40.2)	13±13.1 (1.8-48.2)	16.2±11.8 (1.8-48.2)	1.6±0.7 (0.3-4.3)
C27	20.4±9.2 (6.1-37.1)	13.8±12.5 (2.2-43.5)	17.4±11.2 (2.2-43.5)	4.4±2 (0.6-11.7)
C28	10.6±4.8 (3.2-19.2)	6.9±5.7 (1.5-19.3)	8.9±5.5 (1.5-19.3)	1.4±0.6 (0.3-2.9)
C29	22.3±10.1 (5.9-39.7)	14.3±12.6 (3-39)	18.7±11.9 (3-39.7)	5.2±3.3 (0.4-20.7)
C30	6.8±2.9 (2.2-11.4)	4.5±3.1 (1-9.7)	5.7±3.2 (1-11.4)	1±0.4 (0.2-2)
C31	11.6±4.2 (3.5-17.7)	7.7±5.8 (1.2-18.7)	9.8±5.3 (1.2-18.7)	4.3±3.2 (0.4-20)
C32	6.1±2.6 (1.7-9.3)	3.9±2.6 (0.7-8.2)	5.1±2.8 (0.7-9.3)	0.9±0.4 (0.2-1.7)
C33	5.8±2.7 (1.7-11.5)	3.9±3.1 (0.9-9.6)	4.9±3 (0.9-11.5)	1.8±1.1 (0.1-6.3)
C34	2.1±2.1 (0-5.5)	1.2±1.4 (0-4)	1.7±1.8 (0-5.5)	0.3±0.3 (0-0.9)

300 ^a The unit is ng m⁻³ for all organic compounds and μg m⁻³ for PM_{2.5}, OC, EC and SOC; ^b mean±SD
 301 (min-max); ^c SOC concentration was calculated by EC-tracer method; ^d Haze days: PM_{2.5}≥75 μg
 302 m⁻³; ^e Non-haze days: PM_{2.5}<75 μg m⁻³;

303 **3.2 Chemical Mass Closure (CMC)**

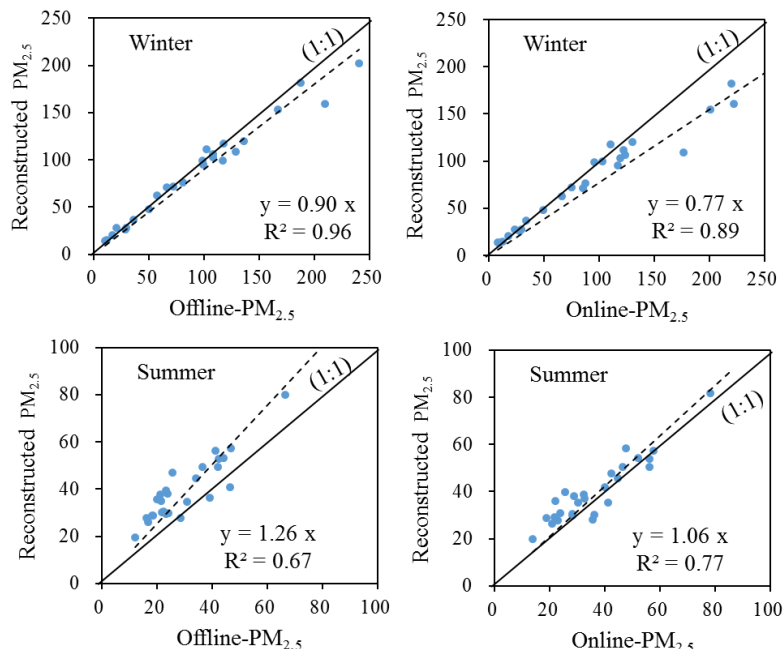
304 The composition of PM_{2.5} applying the chemical mass closure method is plotted in Fig. 2
 305 and summarized in Table S1. Because the gravimetrically measured mass (offline PM_{2.5})
 306 differs slightly from online PM_{2.5} (Fig. S2), the regression analysis results between mass
 307 reconstructed using mass closure (reconstructed PM_{2.5}) and both measured PM_{2.5}
 308 (offline PM_{2.5}/ online PM_{2.5}) were investigated and plotted in Fig. 3.

309



310
311 **Figure 2.** Chemical components of reconstructed PM_{2.5} (offline) applying mass closure method.

312
313



314
315 **Figure 3.** Regression results between reconstructed PM_{2.5} and offline/online PM_{2.5} by chemical mass
316 closure method.

317 As shown in Fig. 3, measured offline/online PM_{2.5} were moderately well correlated
318 with the reconstructed PM_{2.5} with slopes of 0.77~1.26 and R² of 0.67~0.96. In winter,
319 the regression results were good between reconstructed PM_{2.5} and offline-PM_{2.5}. For
320 online-PM_{2.5}, it was much higher than the reconstructed PM_{2.5} when the mass was over
321 170 $\mu\text{g m}^{-3}$. After excluding the outliers (2 outliers of offline-PM_{2.5} > 200 $\mu\text{g m}^{-3}$ and 4
322 outliers of online-PM_{2.5} > 170 $\mu\text{g m}^{-3}$), the regression results improved with both slopes
323 and R² approaching unity (Fig. S3). This could indicate some uncertainties in offline
324 and/or online PM_{2.5} measurement for heavily polluted samples, or the applied OM/OC
325 ratio in winter was not suitable for converting OC to OM in heavily polluted samples.
326 During the summer campaign, the slope of the reconstructed PM_{2.5} and online-PM_{2.5}
327 was close to 1, but that of reconstructed PM_{2.5} and offline-PM_{2.5} was 1.26. This could
328 be due to the loss of semi-volatile compounds from PTFE filters or the positive artefacts

329 of quartz filters for chemical analyses, which can absorb more organics than PTFE
 330 filters that are used for PM weighing. To avoid loss of semi-volatiles, all collected
 331 samples were stored in cold conditions, including during shipment. The datapoints were
 332 more scattered in summer, which could result from the large difference in OM-OC
 333 relationships from day to day. The reconstructed inorganics (reconstructed PM_{2.5}
 334 excluding OM) correlated well with offline-PM_{2.5}, but OM did not (Fig. S4). Hence,
 335 the discrepancies of between reconstructed PM_{2.5} and offline/online PM_{2.5} in summer
 336 may be mainly attributable to variable OM/OC ratios.

337 During the winter campaign, the carbonaceous components (OM & EC) accounted
 338 for 47.2% of total reconstructed PM_{2.5}, followed by the secondary inorganic ions (NH₄⁺,
 339 SO₄²⁻, NO₃⁻) (35.0%). In summer, on the contrary, secondary inorganic salts
 340 represented 45.2% of PM_{2.5} mass, followed by carbonaceous components (35.2%).
 341 Bound water contributed 4.6% and 7.2% of PM_{2.5} during the winter and summer,
 342 respectively. All other components combined accounted for 13.2% and 12.4% of PM_{2.5}
 343 during the winter and summer campaigns, respectively.

344

345 **3.3 Source apportionment of fine OC in urban Beijing applying a CMB model**

346 The CMB model resolved seven primary sources of OC in winter and summer,
 347 including vegetative detritus, straw and wood burning (biomass burning, BB), gasoline
 348 vehicles, diesel vehicles, industrial coal combustion (Industrial CC), residential coal
 349 combustion (Residential CC) and cooking. It explained an average of 75.7% (45.3-
 350 91.3%) and 56.1% (34.3-76.3%) of fine OC in winter and summer, respectively. The
 351 averaged CMB source apportionment results in winter and summer are presented in
 352 Table 2. Daily source contribution estimates to fine OC and the relative abundance of
 353 different sources contributions to OC in winter and summer are shown in Fig. 4.

354 During the winter campaign, coal combustion (industrial and residential CC, 7.5 μg
 355 m^{-3} , 35.0% of OC) was the most significant contributor to OC, followed by Other OC
 356 (5.3 $\mu\text{g m}^{-3}$, 24.8%), biomass (3.8 $\mu\text{g m}^{-3}$, 17.6%), traffic (gasoline and diesel vehicles,
 357 2.6 $\mu\text{g m}^{-3}$, 11.9%), cooking (2.2 $\mu\text{g m}^{-3}$, 10.3%), vegetative detritus (0.09 $\mu\text{g m}^{-3}$, 0.4%).
 358 On winter haze days, industrial coal combustion, cooking and Other OC were
 359 significantly higher (nearly tripled) compared to non-haze days. During the summer
 360 campaign, Other OC (2.9 $\mu\text{g m}^{-3}$, 45.6%) was the most significant contributor to OC,
 361 followed by coal combustion (2.0 $\mu\text{g m}^{-3}$, 31.1%), cooking (0.7 $\mu\text{g m}^{-3}$, 10.3%), traffic
 362 (0.4 $\mu\text{g m}^{-3}$, 6.1%), biomass burning (0.3 $\mu\text{g m}^{-3}$, 5.3%), and vegetative detritus (0.1 μg
 363 m^{-3} , 1.7%).

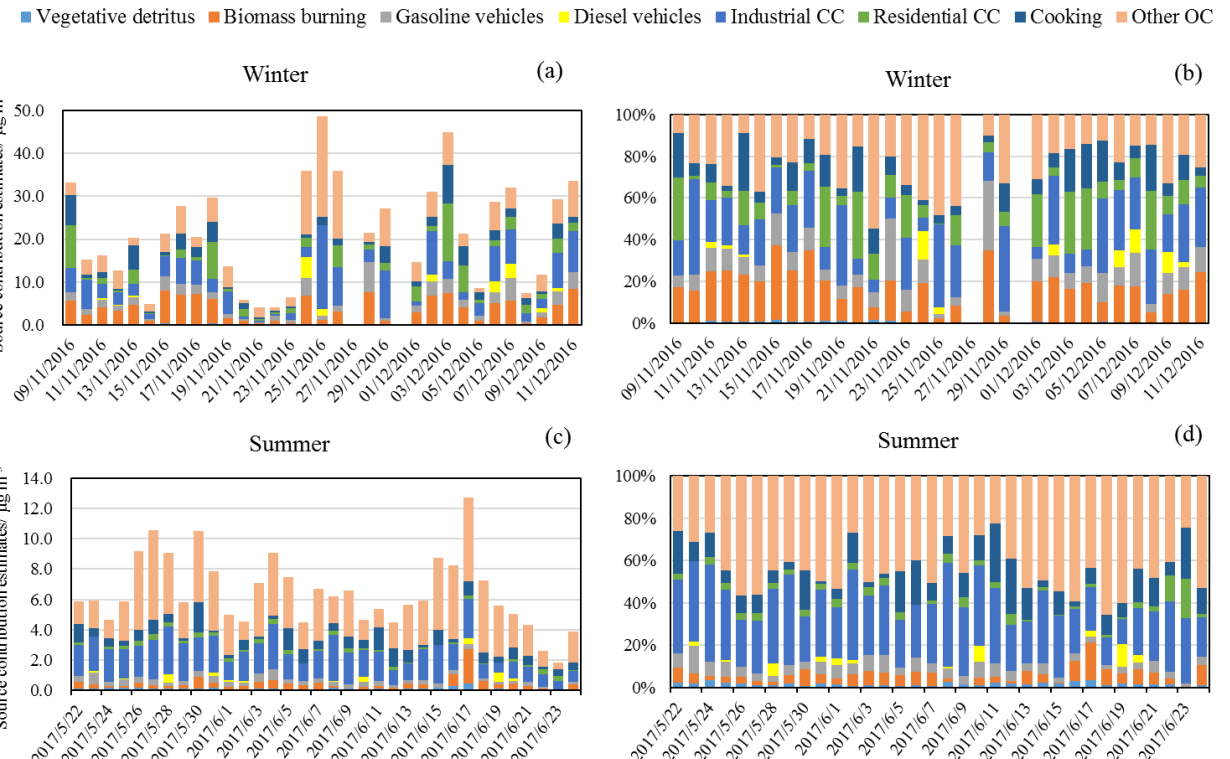
364 **Table 2.** Source contribution estimates (SCE, $\mu\text{g m}^{-3}$) for fine OC in urban Beijing
 365 during winter and summer from the CMB model

Sources	Winter		Winter (n=31)	Summer (n=34)
	Haze (n=18)	Non-haze (n=13)		
Vegetative detritus	0.11 \pm 0.08	0.07 \pm 0.08	0.09 \pm 0.08	0.11 \pm 0.08
Biomass burning	4.80 \pm 2.23	2.38 \pm 2.57	3.78 \pm 2.64	0.34 \pm 0.39
Gasoline vehicles	2.35 \pm 1.27	1.59 \pm 1.85	2.03 \pm 1.56	0.31 \pm 0.16
Diesel vehicles	0.83 \pm 1.43	0.14 \pm 0.33	0.54 \pm 1.15	0.08 \pm 0.16
Industrial coal combustion	7.09 \pm 4.17	1.95 \pm 1.36	4.94 \pm 4.15	1.82 \pm 0.72
Residential coal combustion	3.64 \pm 3.72	1.16 \pm 0.96	2.60 \pm 3.12	0.18 \pm 0.11

Cooking	3.23 \pm 2.30	0.85 \pm 0.52	2.23 \pm 2.13	0.66 \pm 0.43
Other OC ^a	7.4 \pm 5.6	2.5 \pm 1.4	5.3 \pm 4.9	2.9 \pm 1.5
Calculated OC ^b	22.0 \pm 6.5	8.2 \pm 5.3	16.2 \pm 9.1	3.5 \pm 1.2
Measured OC	29.4 \pm 9.2	10.7 \pm 6.2	21.5 \pm 12.3	6.4 \pm 2.3

366 ^a Other OC is calculated by subtracting calculated OC from measured OC;.

367 ^b Calculated OC is the sum of OC from all seven primary sources: vegetative detritus, biomass burning,
368 gasoline vehicles, diesel vehicles, industrial coal combustion, residential coal combustion and cooking.



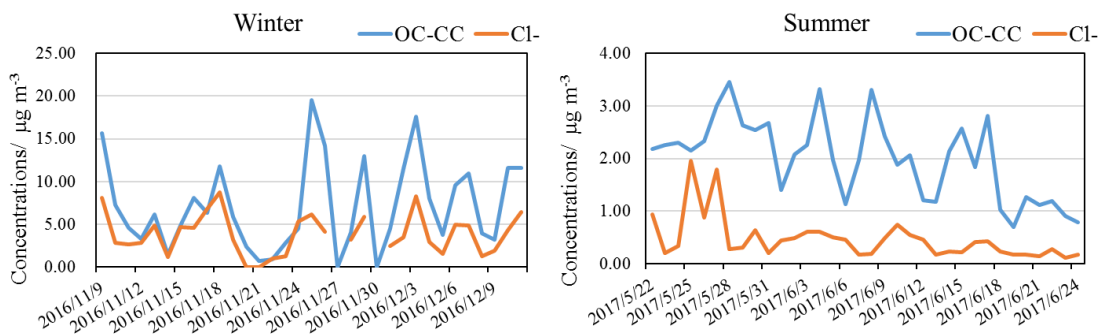
369

370 **Figure 4.** Daily source contribution estimates to fine OC in (a) winter and (c) summer
 371 and their relative abundance in winter (b) and summer (d)

372 3.3.1 Industrial and residential coal combustion

373 In China, a large amount of coal is used in thermal power plant, industries, urban and
 374 rural houses in northern China, especially during the heating period (mid-November to
 375 mid-March) (Huang et al., 2017; Yu et al., 2019). But urban household coal use
 376 experienced a remarkable drop of 58% during 2005-2015, which is much higher than
 377 that of rural household coal use (5% of decrease) (Zhao et al., 2018). In this study, coal
 378 combustion is the single largest source that contributed to primary OC in both winter
 379 and summer. In addition, industrial CC was a more significant source of OC than
 380 residential CC in urban Beijing. On average, coal combustion related OC was 7.5 ± 5.0
 381 $\mu\text{g m}^{-3}$ ($34.5 \pm 9.8\%$ of OC) in winter, which was more than 3 times of that in summer -
 382 $2.0 \pm 0.8 \mu\text{g m}^{-3}$ ($32.3 \pm 10.2\%$ of OC), but the percentage contribution is similar. A
 383 similar seasonal trend was also found in other studies in Beijing (Zheng et al., 2005;
 384 Wang et al., 2009), but the relative contribution of coal combustion was much lower
 385 than in this study. Industrial CC derived OC was 4.94 ± 4.15 and $1.82 \pm 0.72 \mu\text{g m}^{-3}$ in
 386 winter and summer, respectively. Residential CC derived OC was 2.60 ± 3.12 and
 387 $0.18 \pm 0.11 \mu\text{g m}^{-3}$ in winter and summer, respectively. Residential CC was much higher
 388 in winter compared to that in summer. On haze days, industrial CC and residential CC
 389 derived OC were 3.6 and 3.1 times that on non-haze days, respectively, indicating an
 390 important contribution to haze formation from industrial CC.

391 Coal combustion is also a major source for particulate chloride (Chen et al., 2014).
 392 Because Beijing is an inland city, the contribution of marine aerosols to particulate Cl^-
 393 is considered minor, which is also supported by the higher Cl^-/Na^+ mass ratios in winter
 394 (10.1 ± 4.8) and summer (2.7 ± 1.8) than sea water (1.81), indicative of significant
 395 contributions from anthropogenic sources (Bondy et al., 2017). Yang et al. (2018) also
 396 reported that the contribution of sea-salt aerosol to fine particulate chloride was
 397 negligible in China inland areas even during summer. Hence, Cl^- in this study was
 398 mainly from anthropogenic sources. The time series of OC from coal combustion (OC-
 399 CC) and Cl^- during winter and summer of Beijing are shown in Fig. 5. OC-CC and Cl^-
 400 exhibited similar trends in both seasons. The correlation coefficient (R^2) between OC-
 401 CC and Cl^- during winter was 0.62, which could be attributed to enhanced coal
 402 combustion activities in this season. No significant correlation between the two was
 403 found during the summer campaign, indicating the abundance of Cl^- in summer was
 404 more influenced by other sources, probably including biomass burning. In addition, due
 405 to the semi-volatility of ammonium chloride, it is liable to evaporate in summer (Pio
 406 and Harrison, 1987). A similar phenomenon has been observed in Delhi (Pant et al.,
 407 2015).



408

409 **Figure 5.** Time series of OC from coal combustion (OC-CC) and Cl⁻ in winter and
410 summer in Beijing
411

412 **3.3.2 Biomass burning**

413 Biomass burning (BB), including straw and wood burning, is an important source of
414 atmospheric fine OC, which ranked as the second highest primary source of OC, after
415 industrial coal combustion during the winter campaign, and third highest during the
416 summer campaign after industrial CC and cooking. As shown in Fig. 4, the relative
417 abundance of BB derived-OC during the winter campaign is much higher than the
418 summer campaign. BB-derived OC from the CMB results was $3.78 \pm 2.64 \mu\text{g m}^{-3}$ and
419 $0.34 \pm 0.39 \mu\text{g m}^{-3}$ in winter and summer, contributing 17.6% and 5.3% of OC in these
420 two seasons, respectively. These results are lower than those in 2005-2007 Beijing
421 when BB accounted for 26% and 11% of OC in winter and summer, respectively (Wang
422 et al., 2009). The BB-derived OC on winter haze days ($4.80 \pm 2.23 \mu\text{g m}^{-3}$) was
423 approximately double that of non-haze days ($2.38 \pm 2.57 \mu\text{g m}^{-3}$), accounting for 16.3%
424 and 22.2% of OC on haze and non-haze days, respectively.

425 Levoglucosan is widely used as a key tracer for biomass burning emissions (Bhattarai
426 et al., 2019; Cheng et al., 2013; Xu et al., 2019a). Based on a levoglucosan to OC ratio
427 of 8.2 % (Zhang et al., 2007a; Fan et al., 2020), the BB-derived OC was $3.40 \pm 2.09 \mu\text{g}$
428 m^{-3} and $0.32 \pm 0.35 \mu\text{g m}^{-3}$ during the winter and summer campaigns, respectively. These
429 results are comparable to BB-derived OC from the CMB in this study. The estimated
430 BB-derived OC concentration are also comparable with the BB-derived OC during the
431 same sampling periods in Tianjin (Fan et al., 2020), but higher than those at IAP in
432 2013-2014 (Kang et al., 2018).. Both of the studies applied the levoglucosan/OC ratio
433 method to estimate the BB-derived OC although the actual ratio in Beijing air may be
434 very different to 8.2%. The heavily elevated OC concentration in winter compared to
435 summer could be a result of increased biomass burning activities for house heating and
436 cooking in Beijing in addition to the unfavorable dispersion conditions under stagnant
437 weather conditions in the winter.

438 In summer, the total OC concentration was highest on 17th June. The sudden rise of
439 OC on this day was attributed to the enhanced biomass burning activities, which led to
440 the highest level of BB-derived OC and highest BBOC to OC abundance. The
441 levoglucosan concentration on this day was also the highest in summer, which reached
442 172 ng m^{-3} .

443 **3.3.3 Gasoline and diesel vehicles**

444 OC and EC are the key components of traffic emissions (gasoline vehicles & diesel
445 engines) (Chen et al., 2014; Chuang et al., 2016). Traffic related OC, as represented by
446 the total sum of OC from gasoline and diesel vehicles, was 2.4 ± 2.3 and $0.39 \pm 0.22 \mu\text{g}$
447 m^{-3} , and contributed $12.1 \pm 7.8\%$ and $6.1 \pm 3.3\%$ of OC in winter and summer,
448 respectively. These results are lower than the contribution of vehicle emissions to OC
449 (13-20%) in Beijing during 2005 and 2006 (Wang et al., 2009), suggesting traffic
450 emissions may be a less significant contributor to fine OC in the atmosphere in Beijing
451 in 2016/2017. By multiplying by OM/OC factors of 2.39 and 1.47 in winter and summer,
452 respectively, as mentioned in section 2.3, traffic related organic aerosol contributed

453 8.2 \pm 6.5% and 2.3 \pm 1.7% of PM_{2.5} in winter and summer, respectively. The summer
454 result was comparable with the vehicular emissions contribution to PM_{2.5} (2.1%) in
455 summer in Beijing, but higher than that in winter (1.5%) in Beijing estimated by using
456 a PMF model (Yu et al., 2019). Gasoline vehicles dominated the traffic emissions;
457 gasoline vehicle-derived OC was 2.03 \pm 1.56 and 0.31 \pm 0.16 $\mu\text{g m}^{-3}$ in winter and
458 summer, respectively, which are approximately four times than that in winter
459 (0.54 \pm 1.15 $\mu\text{g m}^{-3}$) and summer (0.08 \pm 0.16 $\mu\text{g m}^{-3}$) attributed to diesel vehicles. On
460 haze days, gasoline- and diesel-derived OC were 2.35 \pm 1.27 and 0.83 \pm 1.43 $\mu\text{g m}^{-3}$,
461 respectively, much higher than gasoline- (1.59 \pm 1.85 $\mu\text{g m}^{-3}$) and diesel-derived
462 (0.14 \pm 0.33 $\mu\text{g m}^{-3}$) OC on non-haze days. Even though diesel vehicles played a less
463 important role in OC emissions, diesel-derived OC on haze days increased by around 6
464 times above that of non-haze days, and such an increase was much higher than for
465 gasoline, suggesting a potentially important role of diesel emissions on haze formation.

466 3.3.4 Cooking

467 Cooking is expected to be an important contributor of fine OC in densely populated
468 Beijing, which has a population of over 21 million. The cooking source profile was
469 selected from a study which was carried out in the urban area of another Chinese
470 megacity- Guangzhou, which includes fatty acids, sterols, monosaccharide anhydrides,
471 alkanes and PAHs in particles from the Chinese residential cooking (Zhao et al., 2015).
472 The resultant cooking related OC concentrations were 2.23 \pm 2.13 $\mu\text{g m}^{-3}$ and 0.66 \pm 0.43
473 $\mu\text{g m}^{-3}$ in winter and summer, respectively, and both accounted for about 10% to total
474 OC. Cooking OC was 3.23 \pm 2.30 $\mu\text{g m}^{-3}$ on winter haze days, around four times higher
475 than that on non-haze days (0.85 \pm 0.52 $\mu\text{g m}^{-3}$).

476 3.3.5 Vegetative detritus

477 Vegetative detritus made a minor contribution to fine particle mass. Its concentration
478 was 0.09 \pm 0.08 $\mu\text{g m}^{-3}$ (0.4%) and 0.11 \pm 0.08 $\mu\text{g m}^{-3}$ (1.7%) of OC during the winter and
479 summer campaigns, respectively. These contributions are comparable with that in
480 winter (0.5%), but higher than that in summer (0.3%) in urban Beijing during 2006-
481 2007 (Wang et al., 2009). These results are also higher than the plant debris-derived
482 OC in Tianjin in winter 2016 (0.02 $\mu\text{g m}^{-3}$) and summer 2017 (0.01 $\mu\text{g m}^{-3}$), which were
483 calculated based on the relationship of glucose and plant debris and a OM/OC ratio of
484 1.93 (Fan et al., 2020).

485 3.3.6 Other OC

486 The Other OC was calculated by subtracting the calculated OC (the sum of OC from
487 seven main sources) from measured OC concentrations. As shown in Table S2, there
488 are four major source categories of OC in Beijing based on the Multi-resolution
489 Emission Inventory for China (MEIC), which include power, industry, residential and
490 transportation (Zheng et al., 2018). In the “industry” category, industrial coal
491 combustion has been resolved by the CMB model. The local emissions of OC from
492 industrial coal in Beijing were zero (shown in Table S2), and hence, the resolved POC
493 from industrial coal combustion in Beijing should be regionally-transported. The MEIC
494 data also show a small industrial oil combustion source. Since the tracers for this are
495 likely to be the same as those for petroleum-derived road traffic emissions in CMB, this

496 may result in a small overestimation of the latter source. For the industrial processes
497 related OC which have not been resolved by the CMB model, the annual average OC
498 emissions in Beijing were 1161 and 1083 tonnes in 2016 and 2017 respectively, which
499 accounted for 7.7% and 9.0% of the total OC emissions (POC). Therefore, the
500 contribution from industrial processes to the total OC in the atmosphere (POC+SOC)
501 was considered relatively small. The Other OC in this study is likely to be a mixture of
502 predominantly SOC and a small portion of POC from sources such as industrial
503 processes.

504 The Other OC was 5.3 ± 4.9 and $2.9 \pm 1.5 \mu\text{g m}^{-3}$ in winter and summer, respectively,
505 contributing 24.8% and 43.9% of total measured OC. This is in good agreement with
506 the Other OC estimated by CMB in another study in urban Beijing, for which Other OC
507 contributed 22% and 44% of OC in winter and summer, respectively (Wang et al., 2009).
508 SOC/OC in summer was more than 10% higher than that in summer 2008 in Beijing
509 estimated using a tracer yield method, with the SOC derived from specific VOC
510 precursors (toluene, isoprene, α -pinene and β -caryophyllene) accounting for 32.5% of
511 OC (Guo et al., 2012).

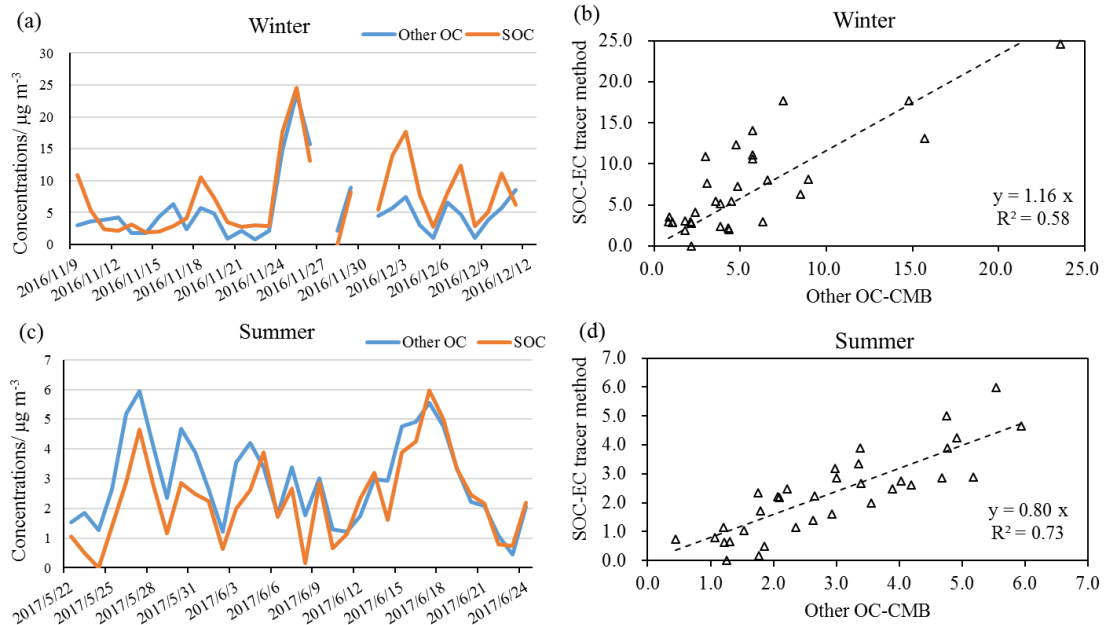
512 Even though the Other OC concentration was lower in summer, its relative
513 abundance was higher than that in winter, suggesting relatively higher efficiency of
514 SOA formation in summer due to more active photochemical processes under higher
515 temperature and strong radiation. The Other OC on winter haze days was $7.4 \pm 5.6 \mu\text{g m}^{-3}$,
516 approximately 3 times of that on non-haze days ($2.5 \pm 1.4 \mu\text{g m}^{-3}$). Other OC is also
517 compared with the SOC estimated by EC-tracer method below.

518 3.3.7 SOC calculated based on the EC-tracer method

519 EC is a primary pollutant, while OC can originate from both primary sources and form
520 in the atmosphere from gaseous precursors, namely primary organic carbon (POC) and
521 SOC, respectively (Xu et al., 2018). The OC/EC ratios can be used to estimate the
522 primary and secondary carbonaceous aerosol contributions. Usually, OC/EC ratios > 2.0 or 2.2 have been applied to identify and estimate SOA (Liu et al., 2017). In this
523 study, all samples were observed with higher OC/EC ratios (> 2.2). SOC in this study
524 was estimated using the equation below, assuming EC comes 100% from primary
525 sources and the OC/EC ratio in primary sources is relatively constant (Turpin and
526 Huntzicker, 1995; Castro et al., 1999):

$$528 \quad \text{SOC}_i = \text{OC}_i - \text{EC}_i \times (\text{OC/EC})_{\text{pri}} \quad (4)$$

529 where SOC_i , OC_i and EC_i are the ambient concentrations of secondary organic
530 carbon, organic carbon and elemental carbon of sample i , respectively. $(\text{OC/EC})_{\text{pri}}$ is
531 the OC/EC ratio in primary aerosols. It is difficult to accurately determining the ratio
532 of $(\text{OC/EC})_{\text{pri}}$ for a given area. $(\text{OC/EC})_{\text{pri}}$ varies with the contributions of different
533 sources and can also be influenced by meteorological conditions (Dan et al., 2004). In
534 this work, $(\text{OC/EC})_{\text{pri}}$ was determined based on the lowest 5% of measured OC/EC
535 ratios for the winter and summer campaigns, respectively (Pio et al., 2011). The average
536 SOC concentrations during summer and winter were calculated and are shown in Table
537 1. Daily concentrations of Other OC estimated by CMB and SOC estimated by the EC-
538 tracer method in winter and summer are plotted in Fig. 6, as well as their correlation
539 relationship.



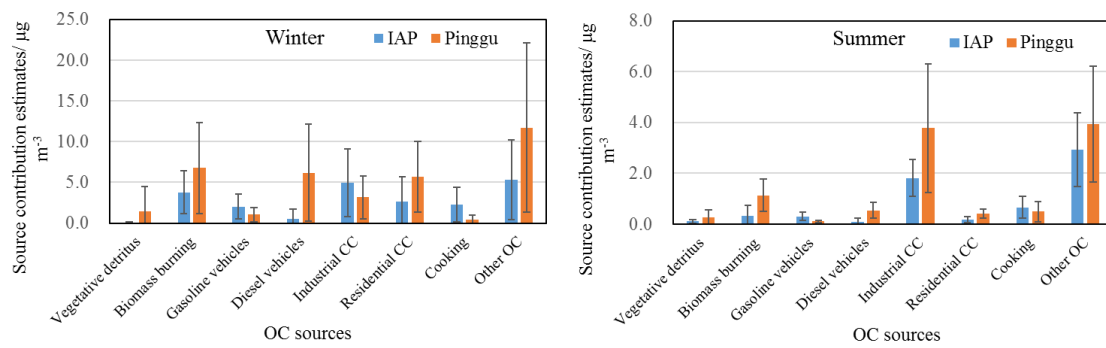
540
 541 **Figure 6.** Time series of mean values for Other OC estimated by CMB and SOC
 542 estimated by the EC-tracer method in winter (a) and summer (c); Correlation
 543 relationship between Other OC estimated by CMB and SOC estimated by the EC-tracer
 544 method in winter (b) and summer (d).

545 The average SOC concentrations in winter and summer are presented in Table 1. The
 546 average SOC concentration during winter was $7.2 \pm 5.7 \mu\text{g m}^{-3}$, accounted for
 547 $36.6 \pm 15.9\%$ of total OC. The average SOC concentration during summer was one third
 548 of that in winter, which was $2.3 \pm 1.4 \mu\text{g m}^{-3}$, accounting for $36.2 \pm 16.0\%$ of total OC.
 549 The mean SOC concentrations during winter haze and non-haze periods were 10.3 ± 5.7
 550 $\mu\text{g m}^{-3}$ and $2.9 \pm 1.4 \mu\text{g m}^{-3}$, contributing to $34.0 \pm 12.0\%$ and $40.5 \pm 20.4\%$ of OC during
 551 haze and non-haze episodes, respectively. As shown in Fig. 6, the SOC estimated by
 552 the EC tracer method followed a similar trend to the Other OC calculated by the CMB
 553 model. They were well-correlated in both seasons with R^2 of 0.58 and 0.73 in winter
 554 and summer samples, respectively and gradients of 1.16 and 0.80. This suggests that
 555 the estimates of Other OC calculated from the CMB outputs were reasonable and
 556 mainly represented the secondary organic aerosol.

557 3.4 Comparison with the source apportionment results in rural Beijing

558 The OC source apportionment results in this study are also compared with those in
 559 another study conducted at a rural site of Beijing - Pinggu during APHH-Beijing
 560 campaigns (Wu et al., 2020). CMB was run based on the results from high-time
 561 resolution PM_{2.5} samples that were collected in Pinggu during the same sampling period,
 562 but not on identical days. It is valuable to study both rural and urban sites, as both
 563 exceed health-based guidelines and require evidence-based mitigation policies which
 564 may differ depending on the source apportionment at each. Furthermore, urban air
 565 pollution may affect the pollution levels in rural areas (Chen et al., 2020b), and
 566 domestic heating and cooking led to high emissions of particles and precursor gases,
 567 which may contribute to air pollution in the cities (Liu et al., 2021). The comparison of
 568 results is presented in Fig. 7 and Table S3.

569 As shown in Fig. 7 and Table S3, slightly more OC was explained by CMB at the
 570 urban site (75.7%) than the rural site (69.1%) during winter, but less OC was explained
 571 at the urban site (56.1%) than the rural site (63.4%) during summer. As at the urban site,
 572 biomass burning and coal combustion are important primary sources in rural Beijing.
 573 Diesel contributed more to OC at the rural site, while cooking contributed more at the
 574 urban site. The rural site also had a larger contribution from vegetative detritus to OC
 575 than the urban site. The source contribution estimates from biomass burning at the rural
 576 site was approximately 2 and 4 times that at the urban site during winter and summer.
 577 In winter, biomass burning contributed a similar percentage of OC at both sites. A
 578 higher percentage of OC from biomass burning was found at the rural site than the
 579 urban site in summer, possibly because of use of biomass for cooking. For traffic
 580 emitted OC, gasoline exceeded diesel at the urban site, while the rural site by contrast
 581 has a larger diesel contribution. Industrial CC emitted OC is higher at the urban site
 582 during winter, but lower in summer compared to the rural site. The source contribution
 583 estimates of residential CC at the urban site is only half that of the rural site in both
 584 seasons, and its relative contribution to OC was also lower at the urban site. Coal is
 585 widely used for cooking and heating at the villages around the rural site at the time of
 586 observations. Cooking accounted for over 10% of OC at the urban site, but less than 5%
 587 at the rural site, which is plausible as the urban site is more densely populated.



588

589 **Figure 7.** Comparison of the source contribution estimates (SCE in $\mu\text{g m}^{-3}$ (%OC)) at
 590 IAP with those at a rural site in Beijing- Pinggu

591 3.5 Comparison with source apportionment results from AMS-PMF

592 Results from AMS-PMF were compared with the CMB source apportionment results
 593 to investigate the consistency and potential uncertainties of both methods, and also to
 594 provide supplemental source apportionment results (Ulbrich et al., 2009; Elser et al.,
 595 2016). Similar comparisons have yielded valuable insights in earlier studies (Aiken et
 596 al., 2009; Yin et al., 2015). It is noteworthy that the CMB model was applied to $\text{PM}_{2.5}$
 597 samples, while AMS-PMF was applied for NR- PM_1 species. This may consequently
 598 cause differences in the chemical composition and source attribution between the two
 599 methods, as larger particles were not captured by AMS. However, as mentioned in the
 600 study of Aiken et al. (2009), the mass concentration between PM_1 and $\text{PM}_{2.5}$ was small
 601 with a reduced fraction of OA and increased fraction of dust. In addition, OC fractions
 602 in fine particles were found mostly concentrated in particles $<1\text{ }\mu\text{m}$ (Chen et al., 2020a;
 603 Zhang et al., 2018; Tian et al., 2020). Hence, the bias was expected to be relatively
 604 small. Six factors in non-refractory (NR)- PM_1 from the AMS were identified based on
 605 the mass spectra measured in winter at IAP by applying a PMF model, including coal
 606 combustion OA (CCOA-AMS), cooking OA (COA-AMS), biomass burning OA

(BBOA-AMS) and 3 secondary factors of oxidized primary OA (OPOA-AMS), less-oxidized OA (LOOOA-AMS), and more-oxidized OA (MOOOA-AMS). In summer, the PMF analysis resulted in 5 factors including 2 primary factors of hydrocarbon-like OA (HOA-AMS), cooking OA (COA-AMS) and 3 secondary factors of oxygenated OA (OOA-AMS): OOA1, OOA2, OOA3. These OOA factors were identified by PMF based on diurnal cycles, mass spectra and the correlations between OA factors and other measured species. Three OOA factors showed significantly elevated O/C ratios (0.67-1.48), and correlated well with SIA ($R=0.52-0.69$). Hence, OOA1, OOA2 and OOA3 represent three types of SOA. Compared to OOA2 and OOA3, OOA1 showed relatively higher f43 (fraction of m/z 43 in OA). In addition, the concentrations of OOA1 and OOA3 were higher in daytime, implying the effect of photochemical processing. The variations of OOA2 tracked well with $C_2H_2O_2^+$ ($R=0.89$), an aqueous-processing related fragment ion (Sun et al., 2016), indicating that OOA2 was an OA factor associated with aqueous-phase processing. Previous studies suggested that aqueous-phase processing plays an important role in the formation of nitrogen-containing compounds (Xu et al., 2017). The fact that OOA2 with relatively high N/C ratios (0.046) was correlated with several N-containing ions (e.g. CH_4N^+ , $C_2H_6N^+$, $R=0.71-0.77$) further supports the above argument. The factor profiles of AMS-PMF in winter and summer are provided in Figs. S5 and S6, respectively.

In order to compare with the source apportionment results of OC in this study from the CMB model, the OA concentrations from the AMS-PMF were converted to OC based on various OA/OC ratios measured in Beijing: 1.35 for CCOA/CCOC (coal combustion organic carbon), 1.31 for HOA/HOC (hydrocarbon-like organic carbon) (Sun et al., 2016), 1.38 for COA/COC (cooking organic carbon), 1.58 for BBOA/BBOC (biomass burning organic carbon) (Xu et al., 2019b), and 1.78 for OOA/OOC (Huang et al., 2010). The concentrations of OA and corresponding OC from AMS-PMF analysis are presented in Table 3. As the AMS data were missing during the period 09th - 15th November 2016, the comparison of the AMS-PMF and CMB results for this period has been excluded.

Table 3. Source contributions of OA and OC ($\mu g m^{-3}$) from AMS-PMF results in urban Beijing during winter and summer

Winter			
Factors	Concentrations/ $\mu g m^{-3}$	Factors	Concentrations/ $\mu g m^{-3}$
CCOA	6.2 \pm 4.4	CCOC	4.6 \pm 3.3
COA	5.9 \pm 4.1	COC	4.3 \pm 3.0
BBOA	6.5 \pm 5.8	BBOC	4.1 \pm 3.7
OPOA	4.6 \pm 2.1	OPOC	2.6 \pm 1.2
LOOOA	5.2 \pm 5.2	LOOOC	2.9 \pm 2.9
MOOOA	8.1 \pm 7.0	MOOOC	4.6 \pm 4.0
OOA ^a	18.0 \pm 13.2	OOC ^d	10.1 \pm 7.4
OM ^b	36.7 \pm 24.0		

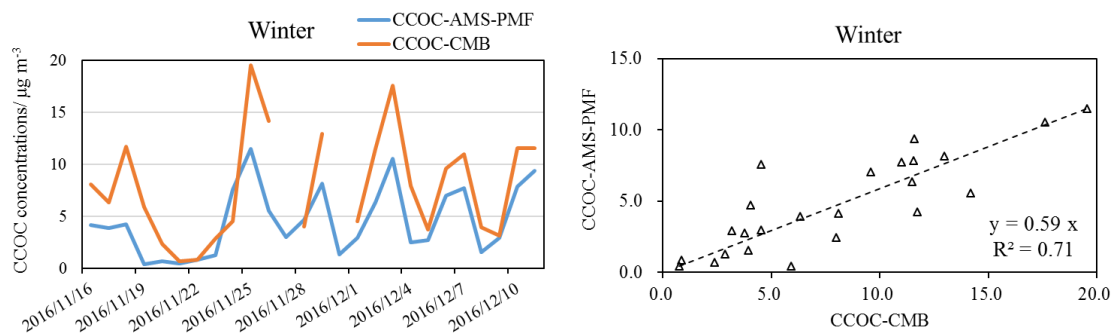
Summer			
Factors	Concentrations/ $\mu g m^{-3}$	Factors	Concentrations/ $\mu g m^{-3}$
HOA	0.7 \pm 0.4	HOC	0.5 \pm 0.3
COA	1.8 \pm 1.0	COC	1.3 \pm 0.7
OOA1	3.3 \pm 1.4	OOC1	1.9 \pm 0.8

OOA2	2.4±2.4	OOC2	1.4±1.3
OOA3	1.9±1.1	OOC3	1.1±0.6
OOA ^c	7.6±3.7	OOC	4.3±2.1
OM	10.1±3.9		

638 ^a *OOA=OPOA+LOOOA+MOOOA*; ^b *OM* is organics measured by AMS; ^c *OOA=OOA1+OOA2+OOA3*;
639 ^d *OOC=OOC1+OOC2+OOC3*

640 The CCOA-AMS factor was mainly characterized by m/z of 44, 73 and 115 (Sun et
641 al., 2016). In winter, CCOA-AMS was $6.2\pm4.4 \mu\text{g m}^{-3}$, contributing 16.9% of OM.
642 CCOC-AMS was $4.6\pm3.3 \mu\text{g m}^{-3}$, which was much lower than the estimated coal
643 combustion OC ($7.9\pm5.2 \mu\text{g m}^{-3}$, industrial and residential coal combustion OC) by
644 CMB (CCOC-CMB). The time series of CCOC-CMB and CCOC-AMS in Fig. 8
645 showed a similar trend with relatively good correlation of $R^2 = 0.71$, but coal
646 combustion estimated by CMB was consistently higher than by AMS-PMF, probably
647 because AMS-PMF only resolved the sources of NR-PM₁, and some coal combustion
648 particles are larger (Xu et al., 2011). The correlation coefficients (R^2) of CCOC-AMS
649 with Cl⁻ and NR-Cl⁻ were 0.49 and 0.65, respectively in the winter data.

650



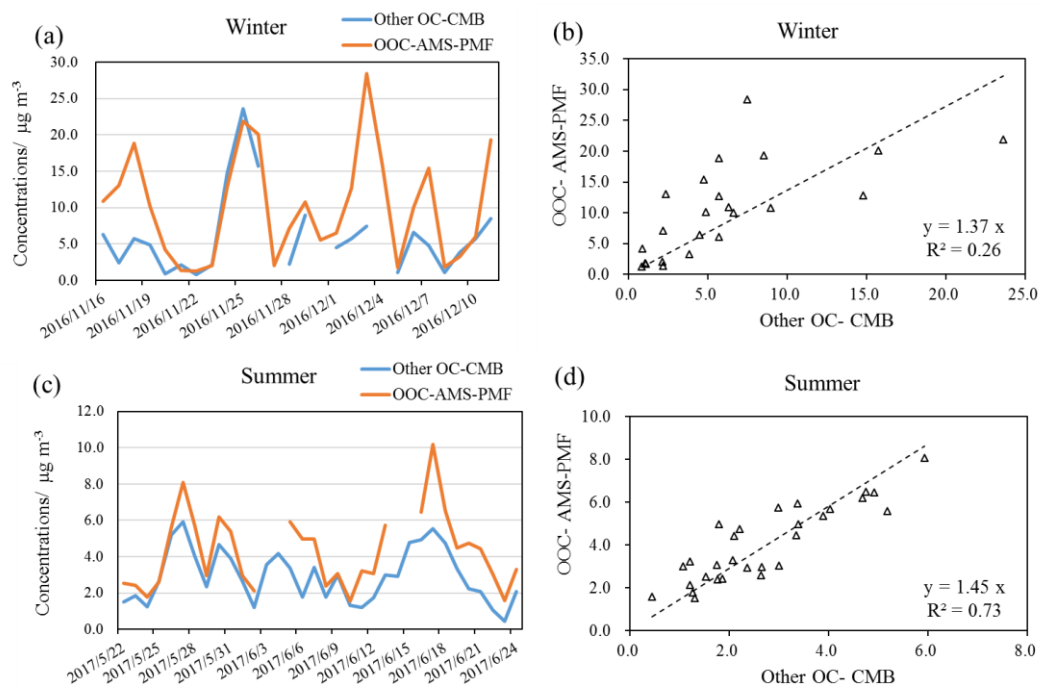
651
652 **Figure 8.** Time series and correlation of coal combustion related OC (CCOC) estimated
653 by CMB and CCOC from AMS-PMF analysis

654 BBOA-AMS in winter was $6.5\pm5.8 \mu\text{g m}^{-3}$, contributing 17.7% of OM. This BBOA-
655 AMS factor included a high proportion of m/z 60 and 73, which are typical fragments
656 of anhydrous sugars like levoglucosan (Srivastava et al., 2019). BBOC-AMS was
657 $4.1\pm3.7 \mu\text{g m}^{-3}$, which was very close to the estimated BBOC-CMB ($3.72\pm2.79 \mu\text{g m}^{-3}$,
658 16.4% of OC) during the same period.

659 COA-AMS is as a common factor identified in both winter and summer results. It is
660 characterized by high m/z of 55 and 57 in the mass spectrum (Sun et al., 2016). COA-
661 AMS was 5.9 ± 4.1 and $1.8\pm1.0 \mu\text{g m}^{-3}$ in winter and summer, respectively, contributing
662 16.1% and 17.8% of OM. COC-AMS was 4.3 ± 3.0 and $1.3\pm0.7 \mu\text{g m}^{-3}$ in winter and
663 summer, respectively, which were almost 2 times of the COC-CMB results for winter
664 ($2.20\pm1.97 \mu\text{g m}^{-3}$) and summer ($0.66\pm0.43 \mu\text{g m}^{-3}$). Yin et al. (2015) also reported that
665 COC-AMS was about 2 times of COC-CMB. The overestimation of cooking OC by
666 AMS-PMF could be due to a low relative ionization efficiency (RIE) for cooking OAs
667 (1.4) in AMS while the actual RIE could be higher, such as 1.56-3.06 (Reyes-Villegas
668 et al., 2018), and/or the use of a relatively low OA/OC ratio for cooking (Xu et al.,
669 2021).

670 HOA-AMS was $0.7 \pm 0.4 \mu\text{g m}^{-3}$ in summer, accounting for 6.9% of OM. HOA-AMS
 671 is usually identified based on the high contribution of aliphatic hydrocarbons in this
 672 factor, particularly m/z of 27, 41, 55, 57, 69 and 71 (Aiken et al., 2009). This result is
 673 lower than that (17% of OM) in rural Beijing during summer 2015 (Hua et al., 2018).
 674 HOC-AMS was $0.5 \pm 0.3 \mu\text{g m}^{-3}$ in summer, which is higher than the traffic
 675 (gasoline+diesel) emitted OC ($0.4 \pm 0.2 \mu\text{g m}^{-3}$) from the CMB model. No obvious
 676 correlation was observed between HOC with nitrate and traffic emitted OC from the
 677 CMB model during summer.

678 OOA-AMS concentrations (the sum of all oxidized OA) were 18.0 ± 13.2 and $7.6 \pm 3.7 \mu\text{g m}^{-3}$ in winter and summer, respectively, accounting for 49.0% and 75.2% of OM.
 679 The derived OOC-AMS concentrations in winter and summer were 10.1 ± 7.4 and
 680 $4.3 \pm 2.1 \mu\text{g m}^{-3}$ in winter and summer, respectively, higher than the Other OC estimated
 681 by CMB (Other OC-CMB) in winter ($6.1 \pm 5.5 \mu\text{g m}^{-3}$) and summer ($2.9 \pm 1.5 \mu\text{g m}^{-3}$) in
 682 this study. This could be because AMS-PMF did not resolve HOC in winter and CCOC
 683 in summer, which may be mixed with the OOA factors and lead to overestimation of
 684 OOC concentrations. The time series and correlation of Other OC-CMB and OOC-
 685 AMS is plotted in Fig. 9. A similar temporal trend was found between them, especially
 686 in summer, which was also observed with a better correlation ($R^2=0.73$).
 687



688
 689 **Figure 9.** Time series of mean values for Other OC estimated by CMB, and OOC
 690 estimated by AMS-PMF in winter (a) and summer (c); Correlation relationship between
 691 Other OC estimated by CMB and OOC estimated by AMS-PMF in winter (b) and
 692 summer (d).

693 In summary, CMB is able to resolve almost all major known primary OA sources, but
 694 AMS-PMF can resolve more secondary OA sources. The AMS-PMF results for major
 695 components, such as CCOC-AMS and OOC-AMS agreed well with the results from
 696 CMB in the winter. However, discrepancies or poor agreement was found for other
 697 sources, such as BBOA-AMS and COA-AMS, although the temporal features were
 698 very similar. Furthermore, AMS-PMF did not identify certain sources, probably due to

699 their relatively small contribution to particle mass. Overall, CMB and AMS-PMF
700 offered complementary data to resolve both primary and secondary sources.

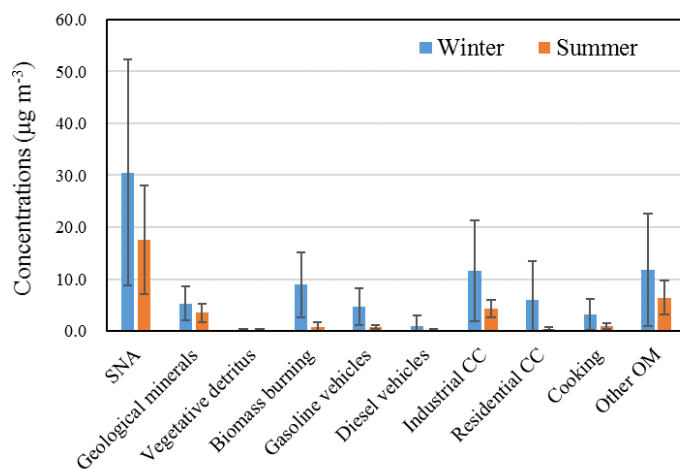
701 **3.6 Source contributions to PM_{2.5} from the CMB model**

702 The source contributions to PM_{2.5} were calculated by multiplication of the fine OC
703 source estimates from CMB by the ratios of fine OC to PM_{2.5} mass (Table S4), which
704 were obtained from the same source profiles used for the OC apportionment by CMB
705 (Zhang et al., 2007b; Wang et al., 2009; Cai et al., 2017; Zhang et al., 2008). For cooking,
706 vegetative detritus and secondary organic aerosols, OM/OC ratios were applied
707 considering the low contribution of inorganic species to PM_{2.5} mass from these sources
708 (Zhao et al., 2007; Bae et al., 2006b). The OM/OC ratios for oxygenated OA were in
709 the range of 1.85-2.3 (Zhang et al., 2005; Aiken et al., 2008), and the OM/OC ratio was
710 2.17 in secondary organic aerosols of PM_{2.5} (Bae et al., 2006a). Therefore, an OM/OC
711 ratio of 2.2 is applied in this study to convert the Other OC to OM. Due to the variability
712 of the OC/PM_{2.5} ratio in the source profiles, the application using the average OC/ PM_{2.5}
713 ratio of each source to convert the OC to PM_{2.5} in all samples may be subject to
714 uncertainties, as both organic species and PM_{2.5} mass measurements are subject to
715 analytical imprecision. Unfortunately, insufficient data are available for a formal
716 analysis of uncertainty, but errors of around +/- 10% seem very probable. In addition,
717 instead of OC/PM_{2.5}, applying an OM/OC ratio to cooking and vegetative detritus
718 sources for the calculation may result in an underestimation of PM_{2.5} source
719 contributions from these sources, because they can also emit inorganic pollutants.
720 However, cooking emissions are mostly organic and the contribution from vegetative
721 detritus to PM_{2.5} is very small, so their effects on source contribution estimation here
722 are considered negligible. The daily PM_{2.5} contribution estimates and seasonal average
723 source contributions are provided in Fig. S7 and Fig. 10, respectively. Detailed data and
724 their relative abundance in the reconstructed PM_{2.5} are summarized in Table S5.

725 As shown in Table S5, PM_{2.5} mass was well explained by those sources which
726 accounted for 91.9±24.1% and 99.0±19.1% of online PM_{2.5} in winter and summer,
727 respectively. In the summer, the offline PM_{2.5} is lower than online observations. Thus,
728 the CMB-based source contributions are more than offline PM_{2.5} mass (121.7±26.6%).
729 On average, the source contributions in winter ranked as SNA > coal combustion >
730 Other OM > biomass burning > gasoline & diesel > geological minerals > cooking >
731 vegetative detritus; in summer these ranked as SNA > other OM > coal combustion >
732 geological minerals > cooking > gasoline & diesel > biomass burning > vegetative
733 detritus.

734 Zheng et al. (2005) investigated the seasonal trends of PM_{2.5} source contributions in
735 Beijing during 2000 applying a CMB model. In winter (January), the contributions from
736 coal combustion, biomass burning, diesel & gasoline, vegetative detritus to PM_{2.5} were
737 9.55 $\mu\text{g m}^{-3}$ (16% of PM_{2.5} and hereafter), 5.8 $\mu\text{g m}^{-3}$ (9%), 3.85 $\mu\text{g m}^{-3}$, 0.33 $\mu\text{g m}^{-3}$,
738 respectively. Contributions from gasoline, diesel, coal combustion and biomass burning
739 were enhanced in Beijing during winter in 2016 compared to 2000, while the
740 contribution from vegetative detritus basically remained similar. In summer (July) 2000,
741 coal combustion contributed 2% of PM_{2.5} (2.39 $\mu\text{g m}^{-3}$), much less than that in summer
742 2016 of this study. The contribution from diesel & gasoline (7.78 $\mu\text{g m}^{-3}$, Zheng et al.,
743 2005) was approximately 10 times of that in 2016 (0.8 $\mu\text{g m}^{-3}$). Similarly, contributions
744 from vegetative detritus and biomass burning were small and insignificant.

745 Zhou et al. (2017) estimated that coal combustion contributions in winter and
 746 summer of Beijing-Tianjin-Hebei area in 2013 were $15.9 \mu\text{g m}^{-3}$ and $2.1 \mu\text{g m}^{-3}$,
 747 respectively, which are comparable with those in this study. These results are also
 748 comparable with the PMF-resolved coal and oil combustion in Beijing during winter
 749 ($17.4 \mu\text{g m}^{-3}$) and summer ($2.2 \mu\text{g m}^{-3}$) in 2010 (Yu et al., 2013). SNA contributed 52.7
 750 and $26.4 \mu\text{g m}^{-3}$ of $\text{PM}_{2.5}$ during winter (January) and summer (July), respectively (Yu
 751 et al., 2013), which are much higher than those in this study. It is noteworthy that a
 752 severe haze pollution event occurred during January 2013, which was characterized by
 753 high concentrations of sulfate and nitrate in several studies (Zhou et al., 2017; Han et
 754 al., 2016). The contribution from biomass burning in winter is consistent ($8.5 \mu\text{g m}^{-3}$)
 755 with this study ($8.9 \mu\text{g m}^{-3}$), but higher in summer ($2.6 \mu\text{g m}^{-3}$) ($0.8 \mu\text{g m}^{-3}$). The
 756 cooking source contributed 4.8 and $1.3 \mu\text{g m}^{-3}$ in $\text{PM}_{2.5}$ during winter and summer 2013,
 757 respectively, which is also comparable with this study.



758

759 **Figure 10.** Seasonal average $\text{PM}_{2.5}$ source contribution estimates from the CMB
 760 model

761

762 **4 Conclusions**

763 Carbonaceous aerosols contributed approximately 59% and 41% of reconstructed $\text{PM}_{2.5}$
 764 in winter and summer at the urban IAP site in Beijing. The OC and EC concentrations
 765 were comparable with more recent studies (Fan et al., 2020; Qi et al., 2018), but lower
 766 than those before 2013 (Yang et al., 2016; Dan et al., 2004), suggesting the
 767 effectiveness of air pollution control measures since 2013 (Vu et al., 2019; Zhang et al.,
 768 2019). CMB modelling showed that in the winter 2016, the top three primary
 769 contributors to $\text{PM}_{2.5}$ -OC were coal combustion (35%), biomass burning (17%), and
 770 traffic (12%); these were in the same order with that at the rural site during the same
 771 study period: coal combustion (29%), biomass burning (18%), and traffic (17%) (Wu
 772 et al., 2020). In the summer 2017, the top three primary contributors to $\text{PM}_{2.5}$ -OC were
 773 coal combustion (32%), cooking (11%), and traffic (6%); these were different to that at
 774 the rural site during the same study period: coal combustion (38%), biomass burning
 775 (11%), and traffic (7%) (Wu et al., 2020). The Other OC, which was well-correlated
 776 ($R^2: 0.6\text{--}0.7$; slope: $0.8\text{--}1.2$) with the secondary OC (SOC) estimated based on the EC-
 777 tracer method, accounted for 25% and 44% of OC at urban site and 31% and 37% of

778 OC at rural site during winter and summer, respectively. Although the annual average
779 PM_{2.5} levels in Beijing reduced from 88 $\mu\text{g m}^{-3}$ in year 2013 to 58 $\mu\text{g m}^{-3}$ in year 2017
780 (Vu et al., 2019), and the deweathered concentration of PM₁ decreased by -38% in 2017
781 comparing to 2007 (Zhang et al., 2020), our CMB modelling results indicate that the
782 coal combustion and biomass burning still remained the dominant primary OC sources
783 in winter 2016 and summer2017, with road traffic ranked as the third highest. Cooking
784 was a more significant source of OC than biomass burning at the urban site during
785 summer. Compared to other CMB studies in Beijing, our study revealed an increase of
786 the contributions from coal combustion, biomass burning and traffic to PM_{2.5} in winter
787 2016 compared to winter 2000, while those in this study remained similar compared to
788 winter 2013. Sulfate, nitrate and ammonium concentrations were significantly lower in
789 this study compared to 2013 (Zheng et al., 2005; Zhou et al., 2017). It is however
790 notable that there is a broad consistency in the findings of the CMB studies, whereas
791 the more numerous studies which have used PMF come to rather diverse conclusions
792 (Srivastava et al., 2020).

793

794 *Data availability.* The data in this article are available from the corresponding authors
795 upon request.

796

797 *Author contributions.* JX did the CMB modelling and drafted the paper with the help
798 of ZS, RMH and all co-authors. DL, TVV conducted the laboratory analysis of organics
799 and inorganics, respectively. XW, YZ provided the CMB source profiles. YS provided
800 the AMS-PMF data.

801

802 *Competing interests.* The authors have no conflict of interests.

803

804 *Acknowledgement.* This research was funded by the UK Natural Environment Research
805 Council (NERC, NE/N007190/1; NE/R005281/1) and Royal Society Advanced
806 Fellowship (grant no: NAF\R1\191220).

807

808 **Reference**

809 Aiken, A. C., DeCarlo, P. F., Kroll, J. H., Worsnop, D. R., Huffman, J. A., Docherty, K. S., Ulbrich, I. M.,
810 Mohr, C., Kimmel, J. R., Sueper, D., Sun, Y., Zhang, Q., Trimborn, A., Northway, M., Ziemann, P. J.,
811 Canagaratna, M. R., Onasch, T. B., Alfarra, M. R., Prevot, A. S. H., Dommen, J., Duplissy, J., Metzger,
812 A., Baltensperger, U., and Jimenez, J. L.: O/C and OM/OC Ratios of Primary, Secondary, and Ambient
813 Organic Aerosols with High-Resolution Time-of-Flight Aerosol Mass Spectrometry, Environ. Sci.
814 Technol., 42, 4478-4485, 10.1021/es703009q, 2008.
815 Aiken, A. C., Salcedo, D., Cubison, M. J., Huffman, J. A., DeCarlo, P. F., Ulbrich, I. M., Docherty, K. S.,
816 Sueper, D., Kimmel, J. R., Worsnop, D. R., Trimborn, A., Northway, M., Stone, E. A., Schauer, J. J.,
817 Volkamer, R. M., Fortner, E., de Foy, B., Wang, J., Laskin, A., Shutthanandan, V., Zheng, J., Zhang, R.,
818 Gaffney, J., Marley, N. A., Paredes-Miranda, G., Arnott, W. P., Molina, L. T., Sosa, G., and Jimenez, J.
819 L.: Mexico City aerosol analysis during MILAGRO using high resolution aerosol mass spectrometry at
820 the urban supersite (T0) – Part 1: Fine particle composition and organic source apportionment, Atmos.

821 Chem. Phys., 9, 6633-6653, 10.5194/acp-9-6633-2009, 2009.
 822 Antony Chen, L. W., Watson, J. G., Chow, J. C., DuBois, D. W., and Herschberger, L.: Chemical mass
 823 balance source apportionment for combined PM2.5 measurements from U.S. non-urban and urban long-
 824 term networks, Atmospheric Environment, 44, 4908-4918,
 825 <https://doi.org/10.1016/j.atmosenv.2010.08.030>, 2010.
 826 Bae, M.-S., Demerjian, K. L., and Schwab, J. J.: Seasonal estimation of organic mass to organic carbon
 827 in PM2.5 at rural and urban locations in New York state, Atmospheric Environment, 40, 7467-7479,
 828 <https://doi.org/10.1016/j.atmosenv.2006.07.008>, 2006a.
 829 Bae, M.-S., Schauer, J. J., and Turner, J. R.: Estimation of the Monthly Average Ratios of Organic Mass
 830 to Organic Carbon for Fine Particulate Matter at an Urban Site, Aerosol Sci. Technol., 40, 1123-1139,
 831 10.1080/02786820601004085, 2006b.
 832 Bhattacharai, H., Saikawa, E., Wan, X., Zhu, H., Ram, K., Gao, S., Kang, S., Zhang, Q., Zhang, Y., Wu, G.,
 833 Wang, X., Kawamura, K., Fu, P., and Cong, Z.: Levoglucosan as a tracer of biomass burning: Recent
 834 progress and perspectives, Atmos. Res., 220, 20-33, <https://doi.org/10.1016/j.atmosres.2019.01.004>,
 835 2019.
 836 Bondy, A. L., Wang, B., Laskin, A., Craig, R. L., Nhliziyo, M. V., Bertman, S. B., Pratt, K. A., Shepson,
 837 P. B., and Ault, A. P.: Inland Sea Spray Aerosol Transport and Incomplete Chloride Depletion: Varying
 838 Degrees of Reactive Processing Observed during SOAS, Environ. Sci. Technol., 51, 9533-9542,
 839 10.1021/acs.est.7b02085, 2017.
 840 Cai, T., Zhang, Y., Fang, D., Shang, J., Zhang, Y., and Zhang, Y.: Chinese vehicle emissions characteristic
 841 testing with small sample size: Results and comparison, Atmospheric Pollution Research, 8, 154-163,
 842 <https://doi.org/10.1016/j.apr.2016.08.007>, 2017.
 843 Castro, L. M., Pio, C. A., Harrison, R. M., and Smith, D. J. T.: Carbonaceous aerosol in urban and rural
 844 European atmospheres: estimation of secondary organic carbon concentrations, Atmospheric
 845 Environment, 33, 2771-2781, [https://doi.org/10.1016/S1352-2310\(98\)00331-8](https://doi.org/10.1016/S1352-2310(98)00331-8), 1999.
 846 Cavalli, F., Viana, M., Yttri, K. E., Genberg, J., and Putaud, J. P.: Toward a standardised thermal-optical
 847 protocol for measuring atmospheric organic and elemental carbon: the EUSAAR protocol, Atmos. Meas.
 848 Tech., 3, 79-89, 10.5194/amt-3-79-2010, 2010.
 849 Chen, C., Zhang, H., Li, H., Wu, N., and Zhang, Q.: Chemical characteristics and source apportionment
 850 of ambient PM1.0 and PM2.5 in a polluted city in North China plain, Atmospheric Environment, 242,
 851 117867, <https://doi.org/10.1016/j.atmosenv.2020.117867>, 2020a.
 852 Chen, L. W. A., Chow, J. C., Wang, X. L., Robles, J. A., Sumlin, B. J., Lowenthal, D. H., Zimmermann,
 853 R., and Watson, J. G.: Multi-wavelength optical measurement to enhance thermal/optical analysis for
 854 carbonaceous aerosol, Atmos. Meas. Tech., 8, 451-461, 10.5194/amt-8-451-2015, 2015a.
 855 Chen, P., Wang, T., Hu, X., and Xie, M.: Chemical Mass Balance Source Apportionment of Size-
 856 Fractionated Particulate Matter in Nanjing, China, Aerosol Air Qual. Res., 15, 1855-1867,
 857 10.4209/aaqr.2015.03.0172, 2015b.
 858 Chen, W.-N., Chen, Y.-C., Kuo, C.-Y., Chou, C.-H., Cheng, C.-H., Huang, C.-C., Chang, S.-Y., Roja
 859 Raman, M., Shang, W.-L., Chuang, T.-Y., and Liu, S.-C.: The real-time method of assessing the
 860 contribution of individual sources on visibility degradation in Taichung, Science of The Total
 861 Environment, 497-498, 219-228, <https://doi.org/10.1016/j.scitotenv.2014.07.120>, 2014.
 862 Chen, Y., Shi, G., Cai, J., Shi, Z., Wang, Z., Yao, X., Tian, M., Peng, C., Han, Y., Zhu, T., Liu, Y., Yang,
 863 X., Zheng, M., Yang, F., Zhang, Q., and He, K.: Simultaneous measurements of urban and rural particles
 864 in Beijing – Part 2: Case studies of haze events and regional transport, Atmospheric Chemistry and
 865 Physics, 20, 9249-9263, 10.5194/acp-20-9249-2020, 2020b.
 866 Cheng, Y., Engling, G., He, K. B., Duan, F. K., Ma, Y. L., Du, Z. Y., Liu, J. M., Zheng, M., and Weber,
 867 R. J.: Biomass burning contribution to Beijing aerosol, Atmospheric Chemistry And Physics, 13, 7765-
 868 7781, 10.5194/acp-13-7765-2013, 2013.
 869 Chow, J. C., Lowenthal, D. H., Chen, L. W. A., Wang, X. L., and Watson, J. G.: Mass reconstruction
 870 methods for PM2.5: a review, Air Quality Atmosphere And Health, 8, 243-263, 10.1007/s11869-015-
 871 0338-3, 2015.
 872 Chuang, M.-T., Chen, Y.-C., Lee, C.-T., Cheng, C.-H., Tsai, Y.-J., Chang, S.-Y., and Su, Z.-S.:
 873 Apportionment of the sources of high fine particulate matter concentration events in a developing
 874 aerotropolis in Taoyuan, Taiwan, Environmental Pollution, 214, 273-281,
 875 <https://doi.org/10.1016/j.envpol.2016.04.045>, 2016.
 876 Dan, M., Zhuang, G., Li, X., Tao, H., and Zhuang, Y.: The characteristics of carbonaceous species and
 877 their sources in PM2.5 in Beijing, Atmospheric Environment, 38, 3443-3452,
 878 <https://doi.org/10.1016/j.atmosenv.2004.02.052>, 2004.
 879 de Miranda, R. M., de Fatima Andrade, M., Dutra Ribeiro, F. N., Mendonça Francisco, K. J., and Pérez-
 880 Martínez, P. J.: Source apportionment of fine particulate matter by positive matrix factorization in the

881 metropolitan area of São Paulo, Brazil, *Journal of Cleaner Production*, 202, 253-263,
882 <https://doi.org/10.1016/j.jclepro.2018.08.100>, 2018.

883 Dong, F.-m., Mo, Y.-z., Li, G.-x., Xu, M.-m., and Pan, X.-c.: [Association between ambient PM10/PM2.5
884 levels and population mortality of circulatory diseases: a case-crossover study in Beijing], *Beijing Da
885 Xue Xue Bao Yi Xue Ban*, 45, 398-404, 2013.

886 Fan, Y., Liu, C. Q., Li, L., Ren, L., Ren, H., Zhang, Z., Li, Q., Wang, S., Hu, W., Deng, J., Wu, L., Zhong,
887 S., Zhao, Y., Pavuluri, C. M., Li, X., Pan, X., Sun, Y., Wang, Z., Kawamura, K., Shi, Z., and Fu, P.: Large
888 contributions of biogenic and anthropogenic sources to fine organic aerosols in Tianjin, North China,
889 *Atmos. Chem. Phys.*, 20, 117-137, 10.5194/acp-20-117-2020, 2020.

890 Fountoukis, C., and Nenes, A.: ISORROPIA II: a computationally efficient thermodynamic equilibrium
891 model for $K^+ - Ca^{2+} - Mg^{2+} - NH_4^+ - Na^+ - SO_4^{2-} - NO_3^- - Cl^- - H_2O$ aerosols, *Atmos. Chem. Phys.*, 7,
892 4639-4659, 10.5194/acp-7-4639-2007, 2007.

893 Fu, P., Zhuang, G., Sun, Y., Wang, Q., Chen, J., Ren, L., Yang, F., Wang, Z., Pan, X., Li, X., and
894 Kawamura, K.: Molecular markers of biomass burning, fungal spores and biogenic SOA in the
895 Taklimakan desert aerosols, *Atmospheric Environment*, 130, 64-73, 10.1016/j.atmosenv.2015.10.087,
896 2016.

897 Guo, S., Hu, M., Guo, Q., Zhang, X., Zheng, M., Zheng, J., Chang, C. C., Schauer, J. J., and Zhang, R.:
898 Primary Sources and Secondary Formation of Organic Aerosols in Beijing, China, *Environ. Sci. Technol.*,
899 46, 9846-9853, 10.1021/es2042564, 2012.

900 Guo, S., Hu, M., Guo, Q., Zhang, X., Schauer, J. J., and Zhang, R.: Quantitative evaluation of emission
901 controls on primary and secondary organic aerosol sources during Beijing 2008 Olympics, *Atmos. Chem.
902 Phys.*, 13, 8303-8314, 10.5194/acp-13-8303-2013, 2013.

903 Han, B., Zhang, R., Yang, W., Bai, Z., Ma, Z., and Zhang, W.: Heavy haze episodes in Beijing during
904 January 2013: Inorganic ion chemistry and source analysis using highly time-resolved measurements
905 from an urban site, *Science of The Total Environment*, 544, 319-329,
906 <https://doi.org/10.1016/j.scitotenv.2015.10.053>, 2016.

907 He, K., Yang, F., Ma, Y., Zhang, Q., Yao, X., Chan, C. K., Cadle, S., Chan, T., and Mulawa, P.: The
908 characteristics of PM2.5 in Beijing, China, *Atmospheric Environment*, 35, 4959-4970,
909 [https://doi.org/10.1016/S1352-2310\(01\)00301-6](https://doi.org/10.1016/S1352-2310(01)00301-6), 2001.

910 Hua, Y., Wang, S., Jiang, J., Zhou, W., Xu, Q., Li, X., Liu, B., Zhang, D., and Zheng, M.: Characteristics
911 and sources of aerosol pollution at a polluted rural site southwest in Beijing, China, *Science of The Total
912 Environment*, 626, 519-527, <https://doi.org/10.1016/j.scitotenv.2018.01.047>, 2018.

913 Huang, R.-J., Zhang, Y., Bozzetti, C., Ho, K.-F., Cao, J.-J., Han, Y., Daellenbach, K. R., Slowik, J. G.,
914 Platt, S. M., Canonaco, F., Zotter, P., Wolf, R., Pieber, S. M., Bruns, E. A., Crippa, M., Ciarelli, G.,
915 Piazzalunga, A., Schwikowski, M., Abbaszade, G., Schnelle-Kreis, J., Zimmermann, R., An, Z., Szidat,
916 S., Baltensperger, U., Haddad, I. E., and Prévôt, A. S. H.: High secondary aerosol contribution to
917 particulate pollution during haze events in China, *Nature*, 514, 218-222, 10.1038/nature13774, 2014.

918 Huang, X., Liu, Z., Liu, J., Hu, B., Wen, T., Tang, G., Zhang, J., Wu, F., Ji, D., Wang, L., and Wang, Y.:
919 Chemical characterization and source identification of PM2.5 at multiple sites in the Beijing-Tianjin-
920 Hebei region, China, *Atmos. Chem. Phys.*, 17, 12941-12962, 10.5194/acp-17-12941-2017, 2017.

921 Huang, X. F., He, L. Y., Hu, M., Canagaratna, M. R., Sun, Y., Zhang, Q., Zhu, T., Xue, L., Zeng, L. W.,
922 Liu, X. G., Zhang, Y. H., Jayne, J. T., Ng, N. L., and Worsnop, D. R.: Highly time-resolved chemical
923 characterization of atmospheric submicron particles during 2008 Beijing Olympic Games using an
924 Aerodyne High-Resolution Aerosol Mass Spectrometer, *Atmos. Chem. Phys.*, 10, 8933-8945,
925 10.5194/acp-10-8933-2010, 2010.

926 Ikemori, F., Uranishi, K., Asakawa, D., Nakatsubo, R., Makino, M., Kido, M., Mitamura, N., Asano, K.,
927 Nonaka, S., Nishimura, R., and Sugata, S.: Source apportionment in PM2.5 in central Japan using positive
928 matrix factorization focusing on small-scale local biomass burning, *Atmospheric Pollution Research*,
929 <https://doi.org/10.1016/j.apr.2021.01.006>, 2021.

930 Kang, M., Ren, L., Ren, H., Zhao, Y., Kawamura, K., Zhang, H., Wei, L., Sun, Y., Wang, Z., and Fu, P.:
931 Primary biogenic and anthropogenic sources of organic aerosols in Beijing, China: Insights from
932 saccharides and n-alkanes, *Environmental Pollution*, 243, 1579-1587,
933 <https://doi.org/10.1016/j.envpol.2018.09.118>, 2018.

934 Le, T.-C., Shukla, K. K., Chen, Y.-T., Chang, S.-C., Lin, T.-Y., Li, Z., Pui, D. Y. H., and Tsai, C.-J.: On
935 the concentration differences between PM2.5 FEM monitors and FRM samplers, *Atmospheric
936 Environment*, 222, 117138, <https://doi.org/10.1016/j.atmosenv.2019.117138>, 2020.

937 Li, L., Ren, L., Ren, H., Yue, S., Xie, Q., Zhao, W., Kang, M., Li, J., Wang, Z., Sun, Y., and Fu, P.:
938 Molecular Characterization and Seasonal Variation in Primary and Secondary Organic Aerosols in
939 Beijing, China, 2018.

940 Li, P., Xin, J., Wang, Y., Wang, S., Li, G., Pan, X., Liu, Z., and Wang, L.: The acute effects of fine particles

941 on respiratory mortality and morbidity in Beijing, 2004–2009, *Environ. Sci. Pollut. Res.*, 20, 6433-6444,
942 10.1007/s11356-013-1688-8, 2013.

943 Li, X., Nie, T., Qi, J., Zhou, Z., and Sun, X. S.: [Regional Source Apportionment of PM2.5 in Beijing in
944 January 2013], *Huan jing ke xue= Huanjing kexue*, 36, 1148-1153, 2015.

945 Liu, B., Wu, J., Zhang, J., Wang, L., Yang, J., Liang, D., Dai, Q., Bi, X., Feng, Y., Zhang, Y., and Zhang,
946 Q.: Characterization and source apportionment of PM2.5 based on error estimation from EPA PMF 5.0
947 model at a medium city in China, *Environmental Pollution*, 222, 10-22,
948 <https://doi.org/10.1016/j.envpol.2017.01.005>, 2017.

949 Liu, L., Zhang, J., Zhang, Y., Wang, Y., Xu, L., Yuan, Q., Liu, D., Sun, Y., Fu, P., Shi, Z., and Li, W.:
950 Persistent residential burning-related primary organic particles during wintertime hazes in North China:
951 insights into their aging and optical changes, *Atmos. Chem. Phys.*, 21, 2251-2265, 10.5194/acp-21-2251-
952 2021, 2021.

953 Liu, Q., Baumgartner, J., Zhang, Y., and Schauer, J. J.: Source apportionment of Beijing air pollution
954 during a severe winter haze event and associated pro-inflammatory responses in lung epithelial cells,
955 *Atmospheric Environment*, 126, 28-35, <https://doi.org/10.1016/j.atmosenv.2015.11.031>, 2016.

956 Oduber, F., Calvo, A. I., Castro, A., Blanco-Alegre, C., Alves, C., Calzolai, G., Nava, S., Lucarelli, F.,
957 Nunes, T., Barata, J., and Fraile, R.: Characterization of aerosol sources in León (Spain) using Positive
958 Matrix Factorization and weather types, *Science of The Total Environment*, 754, 142045,
959 <https://doi.org/10.1016/j.scitotenv.2020.142045>, 2021.

960 Pant, P., Shukla, A., Kohl, S. D., Chow, J. C., Watson, J. G., and Harrison, R. M.: Characterization of
961 ambient PM2.5 at a pollution hotspot in New Delhi, India and inference of sources, *Atmospheric
962 Environment*, 109, 178-189, <https://doi.org/10.1016/j.atmosenv.2015.02.074>, 2015.

963 Paraskevopoulou, D., Liakakou, E., Gerasopoulos, E., Theodosi, C., and Mihalopoulos, N.: Long-term
964 characterization of organic and elemental carbon in the PM_{2.5} fraction: the case of Athens, Greece, *Atmos. Chem. Phys.*, 14, 13313-13325, 10.5194/acp-14-13313-2014, 2014.

965 Pio, C., and Harrison, R.: Vapour pressure of ammonium chloride aerosol: Effect of temperature and
966 humidity, *Atmospheric Environment* (1967), 21, 2711-2715, 10.1016/0004-6981(87)90203-4, 1987.

967 Pio, C., Cerqueira, M., Harrison, R. M., Nunes, T., Mirante, F., Alves, C., Oliveira, C., Sanchez de la
968 Campa, A., Artíñano, B., and Matos, M.: OC/EC ratio observations in Europe: Re-thinking the approach
969 for apportionment between primary and secondary organic carbon, *Atmospheric Environment*, 45, 6121-
970 6132, <https://doi.org/10.1016/j.atmosenv.2011.08.045>, 2011.

971 Qi, M., Jiang, L., Liu, Y., Xiong, Q., Sun, C., Li, X., Zhao, W., and Yang, X.: Analysis of the
972 Characteristics and Sources of Carbonaceous Aerosols in PM(2.5) in the Beijing, Tianjin, and Langfang
973 Region, China, *Int J Environ Res Public Health*, 15, 1483, 10.3390/ijerph15071483, 2018.

974 Rogge, W. F., Hildemann, L. M., Mazurek, M. A., Cass, G. R., and Simoneit, B. R. T.: Sources of fine
975 organic aerosol. 4. Particulate abrasion products from leaf surfaces of urban plants, *Environ. Sci. Technol.*,
976 27, 2700-2711, 10.1021/es00049a008, 1993.

977 Sarnat, J. A., Marmur, A., Klein, M., Kim, E., Russell, A. G., Sarnat, S. E., Mulholland, J. A., Hopke, P.
978 K., and Tolbert, P. E.: Fine Particle Sources and Cardiorespiratory Morbidity: An Application of
979 Chemical Mass Balance and Factor Analytical Source-Apportionment Methods, *Environmental Health
980 Perspectives*, 116, 459-466, doi:10.1289/ehp.10873, 2008.

981 Shi, Z., Vu, T., Kotthaus, S., Harrison, R. M., Grimmond, S., Yue, S., Zhu, T., Lee, J., Han, Y., Demuzere,
982 M., Dunmore, R. E., Ren, L., Liu, D., Wang, Y., Wild, O., Allan, J., Acton, W. J., Barlow, J., Barratt, B.,
983 Beddows, D., Bloss, W. J., Calzolai, G., Carruthers, D., Carslaw, D. C., Chan, Q., Chatzidiakou, L., Chen,
984 Y., Crilley, L., Coe, H., Dai, T., Doherty, R., Duan, F., Fu, P., Ge, B., Ge, M., Guan, D., Hamilton, J. F.,
985 He, K., Heal, M., Heard, D., Hewitt, C. N., Hollaway, M., Hu, M., Ji, D., Jiang, X., Jones, R., Kalberer,
986 M., Kelly, F. J., Kramer, L., Langford, B., Lin, C., Lewis, A. C., Li, J., Li, W., Liu, H., Liu, J., Loh, M.,
987 Lu, K., Lucarelli, F., Mann, G., McFiggans, G., Miller, M. R., Mills, G., Monk, P., Nemitz, E., O'Connor,
988 F., Ouyang, B., Palmer, P. I., Percival, C., Popoola, O., Reeves, C., Rickard, A. R., Shao, L., Shi, G.,
989 Spracklen, D., Stevenson, D., Sun, Y., Sun, Z., Tao, S., Tong, S., Wang, Q., Wang, W., Wang, X., Wang,
990 X., Wang, Z., Wei, L., Whalley, L., Wu, X., Wu, Z., Xie, P., Yang, F., Zhang, Q., Zhang, Y., Zhang, Y.,
991 and Zheng, M.: Introduction to the special issue “In-depth study of air pollution sources and processes
992 within Beijing and its surrounding region (APHH-Beijing)”, *Atmos. Chem. Phys.*, 19, 7519-7546,
993 10.5194/acp-19-7519-2019, 2019.

994 Song, Y., Xie, S., Zhang, Y., Zeng, L., Salmon, L. G., and Zheng, M.: Source apportionment of PM2.5 in
995 Beijing using principal component analysis/absolute principal component scores and UNMIX, *Science
996 of The Total Environment*, 372, 278-286, <https://doi.org/10.1016/j.scitotenv.2006.08.041>, 2006a.

997 Song, Y., Zhang, Y., Xie, S., Zeng, L., Zheng, M., Salmon, L. G., Shao, M., and Slanina, S.: Source
998 apportionment of PM2.5 in Beijing by positive matrix factorization, *Atmospheric Environment*, 40,
999 1526-1537, <https://doi.org/10.1016/j.atmosenv.2005.10.039>, 2006b.

1000

1001 Song, Y., Tang, X., Xie, S., Zhang, Y., Wei, Y., Zhang, M., Zeng, L., and Lu, S.: Source apportionment
1002 of PM_{2.5} in Beijing in 2004, *Journal of Hazardous Materials*, 146, 124-130,
1003 <https://doi.org/10.1016/j.jhazmat.2006.11.058>, 2007.

1004 Srivastava, D., Favez, O., Petit, J. E., Zhang, Y., Sofowote, U. M., Hopke, P. K., Bonnaire, N., Perraudin,
1005 E., Gros, V., Villenave, E., and Albinet, A.: Speciation of organic fractions does matter for aerosol source
1006 apportionment. Part 3: Combining off-line and on-line measurements, *Science of The Total Environment*,
1007 690, 944-955, <https://doi.org/10.1016/j.scitotenv.2019.06.378>, 2019.

1008 Srivastava, D., Xu, J., Liu, D., Vu, T. V., Shi, Z., and Harrison, R. M.: Insight into PM_{2.5} sources by
1009 applying Positive Matrix factorization (PMF) at urban and rural sites of Beijing, *Atmospheric Chemistry
1010 and Physics* (under review), 2020.

1011 Sun, Y., Du, W., Fu, P., Wang, Q., Li, J., Ge, X., Zhang, Q., Zhu, C., Ren, L., Xu, W., Zhao, J., Han, T.,
1012 Worsnop, D. R., and Wang, Z.: Primary and secondary aerosols in Beijing in winter: sources, variations
1013 and processes, *Atmos. Chem. Phys.*, 16, 8309-8329, 10.5194/acp-16-8309-2016, 2016.

1014 Sun, Y., He, Y., Kuang, Y., Xu, W., Song, S., Ma, N., Tao, J., Cheng, P., Wu, C., Su, H., Cheng, Y., Xie,
1015 C., Chen, C., Lei, L., Qiu, Y., Fu, P., Croteau, P., and Worsnop, D. R.: Chemical Differences between
1016 PM₁ and PM_{2.5} in Highly Polluted Environment and Implications in Air Pollution Studies, *Geophysical
1017 Research Letters*, n/a, e2019GL086288, 10.1029/2019gl086288, 2020.

1018 Tian, Y., Feng, Y., Liang, Y., Li, Y., Xue, Q., Shi, Z., Xu, J., and Harrison, R. M.: Size distributions of
1019 inorganic and organic components in particulate matter from a megacity in northern China: dependence
1020 upon seasons and pollution levels (In preparation), 2020.

1021 Turpin, B. J., and Huntzicker, J. J.: Identification of secondary organic aerosol episodes and quantitation
1022 of primary and secondary organic aerosol concentrations during SCAQS, *Atmospheric Environment*, 29,
1023 3527-3544, [https://doi.org/10.1016/1352-2310\(94\)00276-Q](https://doi.org/10.1016/1352-2310(94)00276-Q), 1995.

1024 U.S.EPA: Monitoring PM_{2.5} in ambient air using designated reference or class I equivalent methods, in:
1025 Quality Assurance Handbook for Air Pollution Measurement Systems, 2-12, 2016.

1026 Ulbrich, I. M., Canagaratna, M. R., Zhang, Q., Worsnop, D. R., and Jimenez, J. L.: Interpretation of
1027 organic components from Positive Matrix Factorization of aerosol mass spectrometric data, *Atmos.
1028 Chem. Phys.*, 9, 2891-2918, 10.5194/acp-9-2891-2009, 2009.

1029 Viana, M., Kuhlbusch, T. A. J., Querol, X., Alastuey, A., Harrison, R. M., Hopke, P. K., Winiwarter, W.,
1030 Vallius, M., Szidat, S., Prévôt, A. S. H., Hueglin, C., Bloemen, H., Wåhlin, P., Vecchi, R., Miranda, A. I.,
1031 Kasper-Giebl, A., Maenhaut, W., and Hitzenberger, R.: Source apportionment of particulate matter in
1032 Europe: A review of methods and results, *Journal of Aerosol Science*, 39, 827-849,
1033 <https://doi.org/10.1016/j.jaerosci.2008.05.007>, 2008.

1034 Vu, T. V., Shi, Z. B., Cheng, J., Zhang, Q., He, K. B., Wang, S. X., and Harrison, R. M.: Assessing the
1035 impact of clean air action on air quality trends in Beijing using a machine learning technique,
1036 *Atmospheric Chemistry And Physics*, 19, 11303-11314, 10.5194/acp-19-11303-2019, 2019.

1037 Wang, Q., Shao, M., Zhang, Y., Wei, Y., Hu, M., and Guo, S.: Source apportionment of fine organic
1038 aerosols in Beijing, *Atmos. Chem. Phys.*, 9, 8573-8585, 10.5194/acp-9-8573-2009, 2009.

1039 Wu, X., Chen, C., Vu, T. V., Liu, D., Baldo, C., Shen, X., Zhang, Q., Cen, K., Zheng, M., He, K., Shi, Z.,
1040 and Harrison, R. M.: Source apportionment of fine organic carbon (OC) using receptor modelling at a
1041 rural site of Beijing: Insight into seasonal and diurnal variation of source contributions, *Environmental
1042 Pollution*, 266, 115078, <https://doi.org/10.1016/j.envpol.2020.115078>, 2020.

1043 Xu, J., Jia, C., He, J., Xu, H., Tang, Y.-T., Ji, D., Yu, H., Xiao, H., and Wang, C.: Biomass burning and
1044 fungal spores as sources of fine aerosols in Yangtze River Delta, China – Using multiple organic tracers
1045 to understand variability, correlations and origins, *Environmental Pollution*, 251, 155-165,
1046 <https://doi.org/10.1016/j.envpol.2019.04.090>, 2019a.

1047 Xu, J., Song, S., Harrison, R. M., Song, C., Wei, L., Zhang, Q., Sun, Y., Lei, L., Zhang, C., Yao, X., Chen,
1048 D., Li, W., Wu, M., Tian, H., Luo, L., Tong, S., Li, W., Wang, J., Shi, G., Huangfu, Y., Tian, Y., Ge, B.,
1049 Su, S., Peng, C., Chen, Y., Yang, F., Mihajlidi-Zelić, A., Đorđević, D., Swift, S. J., Andrews, I., Hamilton,
1050 J. F., Sun, Y., Kramawijaya, A., Han, J., Saksakulkrai, S., Baldo, C., Hou, S., Zheng, F., Daellenbach, K.
1051 R., Yan, C., Liu, Y., Kulmala, M., Fu, P., and Shi, Z.: An inter-laboratory comparison of aerosol in organic
1052 ion measurements by Ion Chromatography: implications for aerosol pH estimate, *Atmos. Meas. Tech.
1053 Discuss.*, 2020, 1-36, 10.5194/amt-2020-156, 2020.

1054 Xu, J., Srivastava, D., Wu, X., Hou, S., Vu, Tuan V., Liu, D., Sun, Y., Vlachou, A., Moschos, V., Salazar,
1055 G., Szidat, S., Prévôt, A. S. H., Fu, P., Harrison, R. M., and Shi, Z.: An evaluation of source apportionment
1056 of fine OC and PM_{2.5} by multiple methods: APHH-Beijing campaigns as a case study, *Faraday
1057 Discussions*, 10.1039/D0FD00095G, 2021.

1058 Xu, M., Yu, D., Yao, H., Liu, X., and Qiao, Y.: Coal combustion-generated aerosols: Formation and
1059 properties, *Proceedings of the Combustion Institute*, 33, 1681-1697,
1060 <https://doi.org/10.1016/j.proci.2010.09.014>, 2011.

1061 Xu, W., Sun, Y., Wang, Q., Du, W., Zhao, J., Ge, X., Han, T., Zhang, Y., Zhou, W., Li, J., Fu, P., Wang, Z., and Worsnop, D. R.: Seasonal Characterization of Organic Nitrogen in Atmospheric Aerosols Using High Resolution Aerosol Mass Spectrometry in Beijing, China, *ACS Earth and Space Chemistry*, 1, 673-682, 10.1021/acsearthspacechem.7b00106, 2017.

1062 Xu, W., Sun, Y., Wang, Q., Zhao, J., Ge, X., Xie, C., Zhou, W., Du, W., Li, J., Fu, P., Wang, Z., Worsnop, D. R., and Coe, H.: Changes in Aerosol Chemistry From 2014 to 2016 in Winter in Beijing: Insights From High-Resolution Aerosol Mass Spectrometry, *Journal of Geophysical Research: Atmospheres*, 124, 1132-1147, 10.1029/2018jd029245, 2019b.

1063 Xu, X., Zhang, H., Chen, J., Li, Q., Wang, X., Wang, W., Zhang, Q., Xue, L., Ding, A., and Mellouki, A.: Six sources mainly contributing to the haze episodes and health risk assessment of PM2.5 at Beijing suburb in winter 2016, *Ecotoxicology and Environmental Safety*, 166, 146-156, <https://doi.org/10.1016/j.ecoenv.2018.09.069>, 2018.

1064 Yang, F., Kawamura, K., Chen, J., Ho, K., Lee, S., Gao, Y., Cui, L., Wang, T., and Fu, P.: Anthropogenic and biogenic organic compounds in summertime fine aerosols (PM2.5) in Beijing, China, *Atmospheric Environment*, 124, 166-175, <https://doi.org/10.1016/j.atmosenv.2015.08.095>, 2016.

1065 Yang, X., Wang, T., Xia, M., Gao, X., Li, Q., Zhang, N., Gao, Y., Lee, S., Wang, X., Xue, L., Yang, L., and Wang, W.: Abundance and origin of fine particulate chloride in continental China, *Science of The Total Environment*, 624, 1041-1051, <https://doi.org/10.1016/j.scitotenv.2017.12.205>, 2018.

1066 Yin, J., Cumberland, S. A., Harrison, R. M., Allan, J., Young, D. E., Williams, P. I., and Coe, H.: Receptor modelling of fine particles in southern England using CMB including comparison with AMS-PMF factors, *Atmos. Chem. Phys.*, 15, 2139-2158, 10.5194/acp-15-2139-2015, 2015.

1067 Yu, L., and Wang, G.: Characterization and Source Apportionment of PM2.5 in an Urban Environment in Beijing, *Aerosol Air Qual. Res.*, 13, 10.4209/aaqr.2012.07.0192, 2013.

1068 Yu, L. D., Wang, G. F., Zhang, R. J., Zhang, L. M., Song, Y., Wu, B. B., Li, X. F., An, K., and Chu, J. H.: Characterization and Source Apportionment of PM2.5 in an Urban Environment in Beijing, *Aerosol Air Qual. Res.*, 13, 574-583, 10.4209/aaqr.2012.07.0192, 2013.

1069 Yu, S., Liu, W., Xu, Y., Yi, K., Zhou, M., Tao, S., and Liu, W.: Characteristics and oxidative potential of atmospheric PM2.5 in Beijing: Source apportionment and seasonal variation, *Science of The Total Environment*, 650, 277-287, <https://doi.org/10.1016/j.scitotenv.2018.09.021>, 2019.

1070 Zhang, Q., Worsnop, D. R., Canagaratna, M. R., and Jimenez, J. L.: Hydrocarbon-like and oxygenated organic aerosols in Pittsburgh: insights into sources and processes of organic aerosols, *Atmospheric Chemistry And Physics*, 5, 3289-3311, 10.5194/acp-5-3289-2005, 2005.

1071 Zhang, Q., Zheng, Y., Tong, D., Shao, M., Wang, S., Zhang, Y., Xu, X., Wang, J., He, H., Liu, W., Ding, Y., Lei, Y., Li, J., Wang, Z., Zhang, X., Wang, Y., Cheng, J., Liu, Y., Shi, Q., Yan, L., Geng, G., Hong, C., Li, M., Liu, F., Zheng, B., Cao, J., Ding, A., Gao, J., Fu, Q., Huo, J., Liu, B., Liu, Z., Yang, F., He, K., and Hao, J.: Drivers of improved PM_{2.5} air quality in China from 2013 to 2017, *Proceedings of the National Academy of Sciences*, 116, 24463-24469, 10.1073/pnas.1907956116, 2019.

1072 Zhang, R., Jing, J., Tao, J., Hsu, S. C., Wang, G., Cao, J., Lee, C. S. L., Zhu, L., Chen, Z., Zhao, Y., and Shen, Z.: Chemical characterization and source apportionment of PM_{2.5} in Beijing: seasonal perspective, *Atmos. Chem. Phys.*, 13, 7053-7074, 10.5194/acp-13-7053-2013, 2013.

1073 Zhang, X. Y., Zhuang, G. S., Guo, J. H., Yin, K. D., and Zhang, P.: Characterization of aerosol over the Northern South China Sea during two cruises in 2003, *Atmospheric Environment*, 41, 7821-7836, 10.1016/j.atmosenv.2007.06.031, 2007a.

1074 Zhang, Y.-x., Shao, M., Zhang, Y.-h., Zeng, L.-m., He, L.-y., Zhu, B., Wei, Y.-j., and Zhu, X.-l.: Source profiles of particulate organic matters emitted from cereal straw burnings, *Journal of Environmental Sciences*, 19, 167-175, [https://doi.org/10.1016/S1001-0742\(07\)60027-8](https://doi.org/10.1016/S1001-0742(07)60027-8), 2007b.

1075 Zhang, Y., Schauer, J. J., Zhang, Y., Zeng, L., Wei, Y., Liu, Y., and Shao, M.: Characteristics of Particulate Carbon Emissions from Real-World Chinese Coal Combustion, *Environ. Sci. Technol.*, 42, 5068-5073, 10.1021/es7022576, 2008.

1076 Zhang, Y., Lang, J., Cheng, S., Li, S., Zhou, Y., Chen, D., Zhang, H., and Wang, H.: Chemical composition and sources of PM1 and PM2.5 in Beijing in autumn, *Science of The Total Environment*, 630, 72-82, <https://doi.org/10.1016/j.scitotenv.2018.02.151>, 2018.

1077 Zhang, Y., Vu, T. V., Sun, J., He, J., Shen, X., Lin, W., Zhang, X., Zhong, J., Gao, W., Wang, Y., Fu, T. M., Ma, Y., Li, W., and Shi, Z.: Significant Changes in Chemistry of Fine Particles in Wintertime Beijing from 2007 to 2017: Impact of Clean Air Actions, *Environ. Sci. Technol.*, 54, 1344-1352, 10.1021/acs.est.9b04678, 2020.

1078 Zhao, B., Zheng, H., Wang, S., Smith, K. R., Lu, X., Aunan, K., Gu, Y., Wang, Y., Ding, D., Xing, J., Fu, X., Yang, X., Liou, K.-N., and Hao, J.: Change in household fuels dominates the decrease in PM_{2.5} exposure and premature mortality in China in 2005–2015, *Proceedings of the National Academy of Sciences*, 115, 12401-12406, 10.1073/pnas.1812955115, 2018.

1121 Zhao, X., Hu, Q., Wang, X., Ding, X., He, Q., Zhang, Z., Shen, R., Lü, S., Liu, T., Fu, X., and Chen, L.:
1122 Composition profiles of organic aerosols from Chinese residential cooking: case study in urban
1123 Guangzhou, south China, *Journal of Atmospheric Chemistry*, 72, 1-18, 10.1007/s10874-015-9298-0,
1124 2015.

1125 Zhao, Y., Hu, M., Slanina, S., and Zhang, Y.: Chemical Compositions of Fine Particulate Organic Matter
1126 Emitted from Chinese Cooking, *Environ. Sci. Technol.*, 41, 99-105, 10.1021/es0614518, 2007.

1127 Zheng, B., Tong, D., Li, M., Liu, F., Hong, C., Geng, G., Li, H., Li, X., Peng, L., Qi, J., Yan, L., Zhang,
1128 Y., Zhao, H., Zheng, Y., He, K., and Zhang, Q.: Trends in China's anthropogenic emissions since 2010 as
1129 the consequence of clean air actions, *Atmos. Chem. Phys.*, 18, 14095-14111, 10.5194/acp-18-14095-
1130 2018, 2018.

1131 Zheng, M., Salmon, L. G., Schauer, J. J., Zeng, L., Kiang, C. S., Zhang, Y., and Cass, G. R.: Seasonal
1132 trends in PM2.5 source contributions in Beijing, China, *Atmospheric Environment*, 39, 3967-3976,
1133 <https://doi.org/10.1016/j.atmosenv.2005.03.036>, 2005.

1134 Zhou, J., Xiong, Y., Xing, Z., Deng, J., and Du, K.: Characterizing and sourcing ambient PM2.5 over key
1135 emission regions in China II: Organic molecular markers and CMB modeling, *Atmospheric Environment*,
1136 163, 57-64, <https://doi.org/10.1016/j.atmosenv.2017.05.033>, 2017.

1137 Zhou, W., Wang, Q., Zhao, X., Xu, W., Chen, C., Du, W., Zhao, J., Canonaco, F., Prévôt, A. S. H., Fu, P.,
1138 Wang, Z., Worsnop, D. R., and Sun, Y.: Characterization and source apportionment of organic aerosol at
1139 260 m on a meteorological tower in Beijing, China, *Atmos. Chem. Phys.*, 18, 3951-3968,
1140 10.5194/acp-18-3951-2018, 2018.

1141